
Towards Continuous Sign Language Conversation from Isolated Signs

Youngmin Kim¹ Kyobin Choo¹ Jiwoo Park² Minseo Kim¹
Chanyoung Kim³ Junhyeok Kim¹ Seong Jae Hwang¹

¹Yonsei University ²LG Electronics ³Emory University
winston1214@yonsei.ac.kr

Abstract

Sign language is the primary language for many Deaf and Hard-of-Hearing (DHH) signers, yet most conversational AI systems still mediate interaction through spoken or written language. This spoken-language-centered interface can limit access for signers for whom spoken or written language is not the most accessible medium, motivating direct sign-to-sign conversational modeling. However, sentence-level sign video data are expensive to collect and annotate, leaving existing sign translation and production models with limited vocabulary coverage and weak open-domain generalization. We address this bottleneck by constructing continuous sign conversations from isolated signs: large-scale labeled isolated clips are collected as lexically grounded motion primitives and recomposed into sign-language-ordered utterances derived from existing dialogue corpora. We introduce SIGNAVOX-W, which provides, to our knowledge, the largest labeled isolated-sign vocabulary to date, and SIGNAVOX-U, a continuous 3D sign conversation dataset built from SIGNAVOX-W. To bridge structural mismatch between spoken and signed languages, we use a retrieval-guided spoken-to-gloss translator; to bridge independently collected isolated clips, we propose *BRAID*, a diffusion Transformer that performs duration alignment and co-articulatory boundary inpainting. With the resulting data, we train SIGNAVOX, a direct sign-to-sign conversational model that generates 3D body, hand, and facial motion responses from prior signing context without spoken-language text or externally provided glosses at inference time. Quantitative and qualitative evaluations show improved isolated-to-continuous motion quality, stronger response-level semantic alignment, and scalable signer-centered interaction that better supports visual-spatial articulation.

1 Introduction

Sign language is an independent visual language and serves as the primary means of communication in DHH (Deaf and Hard-of-Hearing) communities [55], functioning as a first language for many of its users. Crucially, however, first-language proficiency in sign language does not imply proficiency in the surrounding spoken or written language. In practice, due to factors such as early language deprivation [23, 46, 4] and limited access to spoken language and literacy support [34, 35], many deaf signers acquire the spoken language as a second language [48, 49, 20]. Therefore, conversational AI systems that rely on spoken or written language may be less accessible to many DHH signers, motivating sign-centered models that interact directly in sign language.

A seemingly straightforward way is to combine sign language translation [7], text-based response generation, and sign language production (SLP) [73, 63, 89] in a cascade. However, the SLP component in such a pipeline remains difficult to scale, since current SLP models are trained on limited

Definitions of sign language terms are provided in Appendix C.

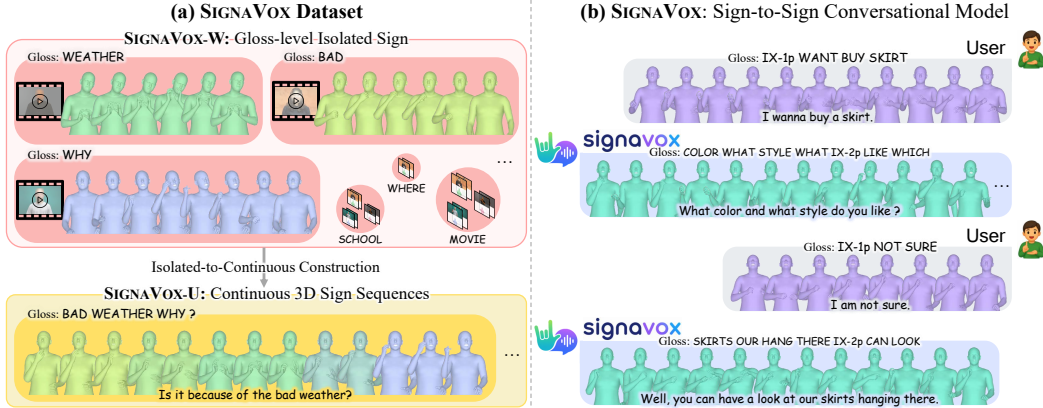


Figure 1: Overview of our proposed dataset and model. (a) We introduce 3D sign language datasets, extending from gloss-level isolated signs (SIGNAVOX-W) to continuous sign sequences (SIGNAVOX-U). (b) We present SIGNAVOX, which generates 3D sign responses from prior signing context.

sentence-level sign data and may generalize poorly to open-domain conversational text. Moreover, this indirect pipeline can obscure visual-spatial structure and timing, and does not directly model how sign responses follow from prior signing context. This motivates direct sign-to-sign response generation, where both context and response are represented as sign motion.

Training sign-to-sign conversational models requires paired data in which prior signing context is followed by a sign response. However, large-scale sign-to-sign conversational datasets are not readily available; existing continuous sign datasets [17, 11, 68] are mostly designed for translation or domain-specific instruction rather than open-ended response generation. We therefore scale data construction by combining abundant text-based dialogue corpora with relatively available labeled isolated-sign datasets: dialogue responses are converted into gloss sequences, and the corresponding isolated signs are composed as lexically grounded motion primitives.

However, constructing sign-to-sign conversational data from isolated signs introduces two key challenges. First, at the visual-motion level, *co-articulatory*¹ *mismatch* arises when independently collected isolated clips are composed into continuous signing. To tackle this, we instantiate our strategy in two steps. We first construct SIGNAVOX-W, a large-scale labeled isolated-sign dataset collected from diverse web sources and public datasets, represented in a shared 3D motion space. Although we retrieve a core-signing clip for each sign unit after trimming non-lexical preparation and retraction motions, adjacent clips remain misaligned in duration, boundary pose, and motion trajectory. Unlike prior works on prepared sign transitions [75, 86], our setting requires composing continuous signing from independently collected clips, making both duration alignment and boundary refinement necessary. We therefore propose **BRAID** (**B**oundary **R**efinement via **co-A**rticulatory **I**npainting **D**iffusion **T**ransformer), which aligns adjacent sign pairs with a predicted duration plan and refines boundary regions through co-articulatory inpainting to produce pseudo-continuous signing.

Second, at the linguistic level, *structural mismatch* arises because spoken and signed languages differ in word order and grammar. We therefore reorder spoken language turns into sign language ordered *gloss*² sequences. To obtain these sequences, we use an LLM-based spoken-to-gloss translator with translation-memory-based RAG [38]. We apply this translator to existing spoken language conversation datasets [36, 12, 42], and transform the resulting gloss sequences into continuous signing with **BRAID** and the isolated signs in SIGNAVOX-W. This results in SIGNAVOX-U, a large-scale sign language conversational dataset represented as sequences of 3D features for training sign-to-sign conversational models.

Building on SIGNAVOX-U, we introduce SIGNAVOX, a sign-to-sign conversational model for sign-centered interaction. SIGNAVOX generates continuous 3D sign motion responses directly from prior signing context and a target role prompt, without routing the interaction through spoken-language text or requiring externally provided gloss sequences at inference time. It models responses

¹Co-articulation refers to neighboring signs influencing each other’s motion.

²Glosses are written labels for signs in sign language order. (e.g., I don’t have any dogs. → DOG I HAVE NONE)

Table 1: Comparison of existing ASL datasets and our SIGNAVOX datasets. In the ‘‘Type’’ column, ‘‘I’’ and ‘‘C’’ denote isolated signing and continuous signing, respectively. Durations marked with * are estimated by converting the reported total number of frames at 25 fps.

Dataset	Vocab.	# Hours	Type	Gloss	Text	Pseudo Annotation	Level
MS-ASL [80]	1K	-	I	✓	-	-	Word
WLASL [39]	2K	-	I	✓	-	-	Word
How2Sign [11]	16K	79	C	✗	✓	-	Sentence
ASLLRP [52]	3,245	2.56	C	✓	✓	-	Single Utterance
OpenASL [68]	3,228	288	C	✗	✓	-	Sentence
YoutubeASL [79]	60K	984	C	✗	✓	-	Sentence
SignAvatar [89]	-	78.8*	I / C	✗	✓	Body, Hand, 2D/3D Keypoints	Word / Sentence
SIGNAVOX-W	42K	79.27	I	✓	✓	Body, Hand, Face	Word
SIGNAVOX-U	22.6K	336.81*	C	✓	✓	Body, Hand, Face	Dialogue

autoregressively in motion blocks with conditional flow-matching heads [45, 78], providing a first step toward sign-centered conversational modeling.

An overview of the proposed dataset and sign-to-sign conversational model is shown in Fig. 1. We evaluate the framework with quantitative metrics and qualitative analyses. *BRAID* improves isolated-to-continuous motion quality, while SIGNAVOX outperforms motion-to-motion baselines in 3D response generation. Together, these results demonstrate that sign-centered conversational modeling can be scaled by combining sign-compatible linguistic planning with real sign motions.

Contributions. Our main contributions are as follows:

- We introduce SIGNAVOX-W and SIGNAVOX-U, a large-scale isolated-sign dataset and a sign-to-sign conversational dataset constructed via spoken-language-to-gloss translation and isolated-to-continuous 3D motion construction.
- We develop *BRAID*, an isolated-to-continuous sign generation model that composes independently collected isolated sign clips into continuous signing through duration alignment and boundary refinement.
- We present, to the best of our knowledge, the first direct sign-to-sign conversational model that takes sign motion as input and generates continuous 3D sign motion responses without text or externally provided gloss sequences at inference time.

2 Related Works

Sign Language Dataset. Sign language processing has long been limited by the lack of large-scale annotated datasets [5]. While many ASL (American Sign Language) isolated-sign datasets have been introduced [80, 39, 9, 2], isolated clips often fail to capture key properties of continuous signing, such as co-articulation [7, 65]. Continuous sign video datasets address this by providing sentence-level data across diverse sign languages [11, 32, 16, 17, 95], but scaling them remains difficult because gloss annotation requires costly expertise. Web-scale datasets mitigate the scale issue [68, 79, 76], yet they typically rely on captions and lack explicit gloss annotations.

Sign Language Processing. Sign language processing has developed largely around recognition, translation, and generation. Recognition predicts the sequence of signs or glosses from continuous signing videos by modeling their temporal progression, often with gloss supervision [10, 94]. Translation maps sign videos into spoken-language sentences, and recent gloss-free methods aim to reduce dependence on costly gloss labels [7, 87, 30, 93, 44, 43]. Generation, or sign language production, synthesizes sign motions from text or gloss inputs, evolving from keypoint-based representations [64, 63] to 3D human models and avatars [89, 97]. Recently, LLMs have also been explored for gloss-free translation [19, 83, 92] and text-conditioned sign production [13, 91].

Co-articulation-Aware Sign Language Modeling. Co-articulation is central to natural continuous signing, yet its influence on the timing and motion of adjacent signs often blurs temporal boundaries, making it a key challenge for modeling continuous sign language [1, 65, 81, 47]. In sign language generation, this challenge is instead framed as the explicit synthesis of co-articulation, where keypoint or mesh-based models learn motion deformation and temporal continuity between adjacent signs [97, 89, 65]. A more specific line of transition-generation methods focuses on transition poses between adjacent segments to alleviate abrupt motion, rather than regenerating entire sign segments [75, 86].

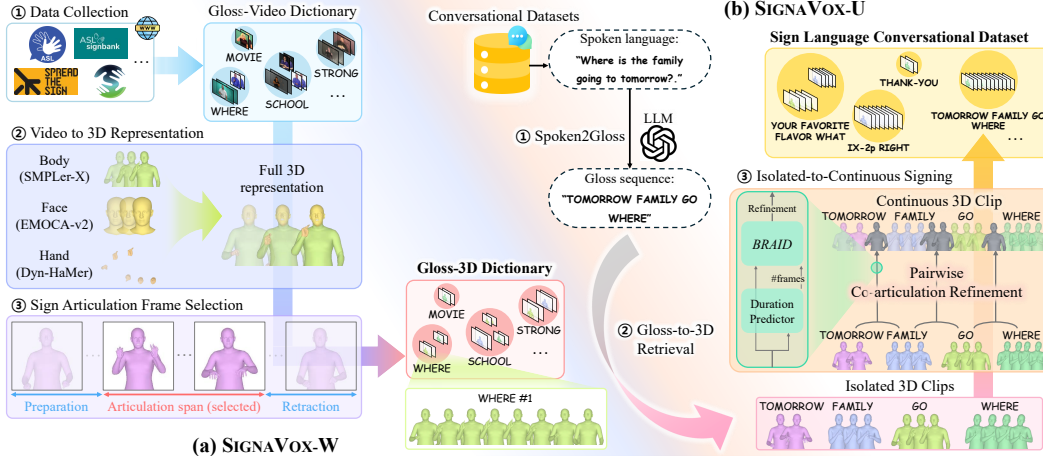


Figure 2: Overall data collection and processing pipeline. (a) illustrates the collection process for our isolated sign language dataset, SIGNAVOX-W. (b) details the construction of SIGNAVOX-U, a conversational dataset created by synthesizing continuous sentences from SIGNAVOX-W.

3 SIGNAVOX Dataset

In this section, we introduce (1) the construction pipeline of SIGNAVOX-W, a large-scale isolated sign clips collected from diverse sources (Sec. 3.1), (2) an overview of our isolated-to-continuous signing model, which converts isolated sign clips into continuous sign sequences with natural co-articulation (Sec. 3.2), and (3) the construction of SIGNAVOX-U, an utterance-level continuous sign dataset built on these two components, enabling broad utterance coverage for improved generality (Sec. 3.3).

3.1 Isolated Sign Dataset Construction

We construct SIGNAVOX-W, a large-scale sign video lexicon with canonical gloss labels for scalable sign language conversation modeling. Table 1 summarizes dataset statistics in comparison to existing ASL datasets, and Fig. 2-(a) illustrates the overall collection and preprocessing pipeline.

Data Collection. Following previous studies [65, 97], we construct a video–gloss dictionary. To ensure generality, we collect data from four web-based sign language dictionaries [70, 27, 67, 25] that provide sign demonstrations performed by native signers, as well as two public datasets [80, 39], rather than relying on a single dataset, thereby achieving broad vocabulary coverage. This results in a one-to-many mapping, where each gloss is associated with multiple video samples. Details of our dataset are provided in the Appendix D.

3D Representation. To mitigate spatial misalignment and domain shifts inherent in multi-source videos, we adopt a normalized 3D representation. Following [89, 31], we estimate part-specific 3D parameters for the body, hands, and face to explicitly capture fine-grained manual and non-manual cues. We estimate full-body motion using SMPLer-X [6] with SMPL-X parameters [57], model hand articulations via Dyn-HaMR [90] based on MANO [62], and estimate facial expressions using EMOCA-v2 [14] based on FLAME [41]. For each gloss clip g_k , we represent its t -th frame using a unified 3D motion feature vector that concatenates body, face, and hand parameters. Specifically,

$$\mathbf{x}_t^{(k)} = [\theta_t^{\text{body}}; \psi_t; \theta_t^{\text{jaw}}; \theta_t^{\text{rhand}}; \theta_t^{\text{lhand}};] \in \mathbb{R}^D. \quad (1)$$

where $D = 206$. Accordingly, the frame-wise motion representation of g_k is denoted as $\mathbf{X}^{(k),\text{raw}} = [\mathbf{x}_1^{(k),\text{raw}}, \dots, \mathbf{x}_{T_k}^{(k),\text{raw}}] \in \mathbb{R}^{T_k \times D}$, where T_k is the number of frames in g_k .

Sign Articulation Frame Selection. Modeling natural co-articulation in sign language videos requires identifying frames that correspond to the core lexical articulation of each sign [65]. We introduce a coarse-to-fine articulation-frame selection pipeline to isolate the core articulation while discarding preparation and retraction segments. First, we perform feature-based coarse boundary estimation to remove long non-signing intervals and narrow each isolated sign clip to its effective signing region. Given an isolated sign clip represented as motion features $\mathbf{X}^{(k),\text{raw}}$, we estimate a frame-wise motion-energy signal from smoothed temporal derivatives and combine it with arm-

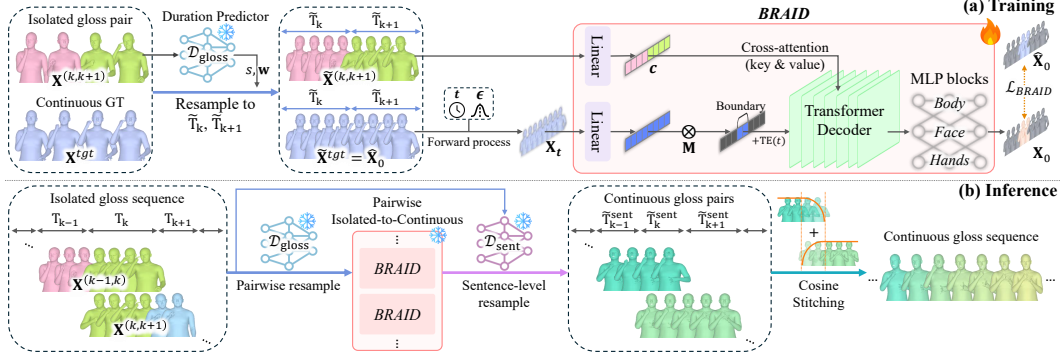


Figure 3: Overview of the *BRAID* framework. (a) The training pipeline of our proposed model. (b) The inference process for generating the sentence-level continuous sign language.

posture gating to suppress low-activity arm-down segments. The resulting signal is used to estimate coarse temporal boundaries (s_k, e_k) , which are further refined in the next stage.

Based on the estimated coarse boundaries (s_k, e_k) , we crop the corresponding video segment and apply a two-stage VideoLLM-based [3] refinement procedure to identify the core lexical articulation. To facilitate more accurate temporal reasoning, we adopt a visual prompting strategy [69, 84] that explicitly overlays frame indices on each frame [37] (e.g., “frame #01”). In the first stage, the model predicts a contiguous articulation span (\hat{s}_k, \hat{e}_k) , which provides an initial estimate of the articulation interval. In the second stage, we present a candidate-focused clip centered around the predicted span and further refine its boundaries by removing residual non-signing segments. For fingerspelled cases such as alphabet letters, where a single canonical handshape is often sufficient, we select one representative frame. As a result, the final articulation-preserving representation is obtained as $\mathbf{X}_{\hat{s}_k:\hat{e}_k}^{(k),\text{raw}}$ or single-frame feature. In the following section, we notate $\mathbf{X}_{\hat{s}_k:\hat{e}_k}^{(k),\text{raw}} \in \mathbb{R}^{(\hat{e}_k - \hat{s}_k + 1) \times D}$ as $\mathbf{X}^{(k)} \in \mathbb{R}^{T_k \times D}$, and define the adjacent gloss-pair sequence as $\mathbf{X}^{(k,k+1)}$ as $[\mathbf{X}^{(k)}; \mathbf{X}^{(k+1)}]$.

3.2 Isolated-to-Continuous Signing

In this section, we describe our pipeline for composing sentence-level signing from isolated clips in SIGNAVOX-W. Since directly concatenating isolated signs leads to temporal and articulatory mismatch at gloss boundaries, we process adjacent gloss pairs with *BRAID* (Boundary Refinement via co-Articulatory Inpainting Diffusion Transformer) and stitch the refined outputs into a continuous signing sequence. The overall pipeline is shown in Fig. 3.

Data Setting. We construct training pairs by using ASLLRP [52] as continuous signing supervision. After organizing ASLLRP into sentence-level utterances with normalized gloss labels, we retrieve corresponding isolated clips from SIGNAVOX-W and compose pseudo sentence-level sequences by sampling one clip per gloss. We repeat this process $n = 14$ times for diversity and decompose the composed sequences into adjacent gloss pairs for training.

Duration Prediction. As shown in Fig. 4, the gloss-pair inputs exhibit a substantial length mismatch with the target continuous segments. Specifically, the input sequences are not only longer on average than the targets, but also display considerably larger variance. This indicates that redundant temporal content still remains around gloss boundaries even after articulation-frame selection. To reduce this discrepancy, we use two duration predictors, denoted by $\mathcal{D}_{\text{gloss}}$ and $\mathcal{D}_{\text{sent}}$. $\mathcal{D}_{\text{gloss}}$ reduces *BRAID*’s refinement burden by adjusting local gloss-pair durations, while $\mathcal{D}_{\text{sent}}$ provides a consistent temporal plan for stitching pairwise outputs into full sentences. Let T_{src} denote the length of the input motion sequence and T_{tgt} its corresponding target length. The predictor estimates a global scale $s = \log(T_{\text{tgt}}/T_{\text{src}})$ and a gloss-wise duration ratio $\mathbf{w} = [w_1, \dots, w_K]$, where K denotes the

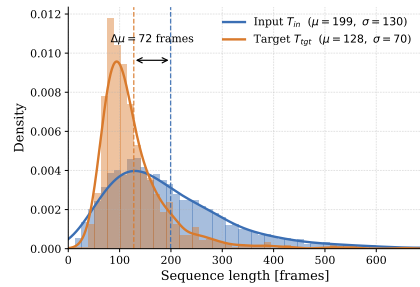


Figure 4: Distribution of sequence lengths for composed gloss-pair inputs and target continuous segments.

number of glosses. The length assigned to the k -th gloss is then computed as $\tilde{T}_k = w_k T_{\text{src}} e^s$. We train the predictor to match the target global scale and gloss-wise duration allocation, using a quantile objective for the scale term to discourage excessive temporal compression. Additional architecture and training details are provided in Appendix F.3.

Architecture. Inspired by MDM [77], we propose *BRAID*, a conditional diffusion Transformer that refines gloss-pair motion sequences into continuous signing. By focusing on boundary regions, *BRAID* restores natural transitions and fine-grained co-articulatory motion. We first perform duration-aware temporal alignment to reduce length mismatch and establish the temporal scale before diffusion-based boundary refinement. The frozen duration predictor $\mathcal{D}_{\text{gloss}}$ estimates target durations \tilde{T}_k and \tilde{T}_{k+1} for the gloss-pair sequence $\mathbf{X}^{(k,k+1)}$. After predicting \tilde{T}_k and \tilde{T}_{k+1} , we linearly resample the two gloss-motion segments to the corresponding durations and concatenate them to obtain the duration-adjusted sequence $\tilde{\mathbf{X}}^{(k,k+1)} \in \mathbb{R}^{(\tilde{T}_k + \tilde{T}_{k+1}) \times D}$. The concatenation point at index \tilde{T}_k defines the boundary between the two resampled gloss segments. Around this boundary, we construct a binary temporal inpainting mask $\mathbf{M} \in \{0, 1\}^{\tilde{T}_k + \tilde{T}_{k+1}}$ as follows:

$$M_i = \mathbf{1} \left[|i - \tilde{T}_k| \leq r \right], \quad r \sim \mathcal{U}\{r_{\min}, \dots, r_{\max}\}. \quad (2)$$

Frames with $M_i = 1$ form the co-articulatory inpainting region, where the denoiser output is used for refinement and receives supervision during training. Frames with $M_i = 0$ serve as temporal context and are preserved from the duration-adjusted input sequence in the final composition.

During training, we use the matched continuous ground-truth pair \mathbf{X}^{tgt} as supervision. To match the length of the duration-adjusted pseudo sequence, we resample it to the same predicted durations, obtaining the duration-aligned target $\tilde{\mathbf{X}}^{\text{tgt}}$, which we denote as the clean target \mathbf{X}_0 . We then corrupt only \mathbf{X}_0 with the standard DDPM forward process [26] at timestep t , producing the noisy target \mathbf{X}_t , while the duration-adjusted pseudo sequence $\tilde{\mathbf{X}}^{(k,k+1)}$ remains clean. The noisy target \mathbf{X}_t is linearly projected as the decoder target stream, while the clean pseudo sequence is projected into conditioning tokens $\mathbf{c} = \phi_c(\tilde{\mathbf{X}}^{(k,k+1)})$, which serve as the key and value memory for cross-attention. The denoiser G_θ is implemented as a RoPE-based [74] Transformer decoder. Given \mathbf{X}_t , timestep t , conditioning tokens \mathbf{c} , and the inpainting mask \mathbf{M} , it predicts the clean motion $\hat{\mathbf{X}}_0 = G_\theta(\mathbf{X}_t, t, \mathbf{c}, \mathbf{M})$. The Transformer decoder output is passed to part-specific MLP heads for body, face, and hands, whose outputs are concatenated to produce the clean-motion prediction $\hat{\mathbf{X}}_0$.

Training. We train *BRAID* with a masked objective consisting of a part-weighted reconstruction loss $\mathcal{L}_{\text{recon}}$ and a velocity regularization \mathcal{L}_{vel} on first-order temporal differences:

$$\mathcal{L}_{\text{braid}} = w(t) \left(\mathcal{L}_{\text{recon}}(\hat{\mathbf{X}}_0, \mathbf{X}_0; \mathbf{M}, \boldsymbol{\omega}_{\text{part}}) + \lambda_{\text{vel}} \mathcal{L}_{\text{vel}}(\Delta \hat{\mathbf{X}}_0, \Delta \mathbf{X}_0; \mathbf{M}^\Delta, \boldsymbol{\omega}_{\text{part}}) \right). \quad (3)$$

Here, $w(t)$ denotes the Min-SNR weighting [24] at diffusion step t , $\boldsymbol{\omega}_{\text{part}}$ is a part-wise feature weight vector that emphasizes hand and face dimensions, and \mathbf{M}^Δ denotes the temporal-difference mask for the velocity term. Detailed definitions of $\mathcal{L}_{\text{recon}}$ and \mathcal{L}_{vel} are provided in the Appendix.

Inference. At inference, we first use $\mathcal{D}_{\text{gloss}}$ to predict pair-level durations for each adjacent gloss pair. Each pair is resampled accordingly and refined through the DDIM reverse process [71] using a symmetric boundary inpainting mask, while the $M_i = 0$ frames are preserved from the duration-adjusted input. In parallel, $\mathcal{D}_{\text{sent}}$ predicts a sentence-level duration plan $\tilde{\mathbf{T}}^{\text{sent}}$. The refined pairwise outputs are split at their predicted gloss boundary, assembled into a sentence-level trajectory, and cosine-fused where intermediate glosses overlap. Finally, the stitched sequence is rescaled gloss-wise to match $\tilde{\mathbf{T}}^{\text{sent}}$, resulting in $\hat{\mathbf{X}}^{\text{sent}} \in \mathbb{R}^{\sum_k \tilde{\mathbf{T}}^{\text{sent}} \times D}$.

3.3 SIGNAVOX-U

Spoken Language to Gloss. To build SIGNAVOX-U, we employ an LLM-based spoken language-to-gloss converter, following prior works [13, 91, 22]. To ensure notation consistency, we adopt the SignStream annotation convention [51] used in ASLLRP [52] as the canonical standard, and guide the LLM with a translation-memory-based RAG strategy. During retrieval, we apply NER-based anonymization to reduce similarity distortions caused by proper nouns.

Retrieval is performed in two stages. First, we compute BM25 [61] and SPLADE [15] scores, and combine them into a hybrid retrieval score after min-max normalization, using weights α and $1 - \alpha$, respectively. Next, we rerank the top candidates using a cross-encoder [85], and combine the reranking

score with the hybrid retrieval score to obtain the final retrieval score. Finally, we select the top-6 examples and incorporate them into the translation-memory prompt, enabling the LLM to generate gloss sequences that better conform to the target annotation convention.

Sign Language Conversational Dataset. To build SIGNAVOX-U, our sign language conversational dataset, we convert existing spoken-language daily conversation datasets [36, 12, 42] into sign language. As illustrated in Fig. 2-(b), this construction pipeline combines a spoken-language-to-gloss translation approach with our developed *BRAID* to transform full conversations into sign sequences. Each conversation is ultimately represented as a sequence of 3D features, allowing us to construct a large-scale sign language conversational dataset. The overall statistics of SIGNAVOX-U are summarized in Table 1, and details can be found in Appendix D.

4 Sign Language Conversational Model

We introduce SIGNAVOX, a sign-to-sign conversational model, trained on SIGNAVOX-U. Details are provided in Appendix H.

Architecture. Inspired by MAR [40], SIGNAVOX autoregressively generates sign responses as fixed-length 3D motion blocks. Given a sign history H_t and a target role prompt r_t , the response $Y_t = [B_1, \dots, B_L]$, with each B_ℓ containing K frames, is factorized as

$$p(Y_t | H_t, r_t) = \prod_{\ell=1}^L p(B_\ell | H_t, r_t, B_{<\ell}), \quad (4)$$

where B_ℓ denotes the ℓ -th motion block. The history H_t is serialized with role and boundary tokens in a ChatML-style layout.

A Transformer decoder maps the serialized history and previous blocks to a conditioning memory, $C_\ell = f_\theta^{\text{dec}}(H_t, r_t, B_{<\ell})$, which conditions the flow heads for the next block. The next block is generated by anatomy-factorized conditional flow-matching heads for the body, face, and hands [45, 78], with a higher-capacity hand head to better model lexical articulation.

To model response structure, SIGNAVOX predicts a boundary state b_ℓ for each block, indicating whether it terminates a sentence, terminates a turn, or contains no boundary. This prediction is distinct from the boundary tokens used for input serialization. For gloss-level semantic planning, SIGNAVOX includes an auxiliary branch that predicts a gloss distribution P_ℓ^{plan} from C_ℓ , without taking gloss sequences as input. We augment the decoder memory with these planning signals:

$$\tilde{C}_\ell = C_\ell + e_{\text{bdry}}(b_\ell) + \alpha_s \phi_{\text{plan}}(P_\ell^{\text{plan}}), \quad (5)$$

where e_{bdry} is a learned boundary-state embedding, ϕ_{plan} maps the soft gloss-plan distribution to the decoder hidden space, and α_s is a curriculum weight. The flow heads are conditioned on \tilde{C}_ℓ to generate the next block.

Training Objectives. We train SIGNAVOX with objectives for motion generation, response structure, and gloss-level semantic planning. The main objective is the conditional flow-matching loss \mathcal{L}_{FM} , computed over the body, face, and hand heads. For response structure, $\mathcal{L}_{\text{bdry}}$ supervises sentence-end and turn-end prediction, with a lightweight calibration term for boundary frequency. For gloss-level semantic planning, $\mathcal{L}_{\text{plan}}$ provides auxiliary CTC supervision by predicting the training gloss sequence from the decoder state prior to motion generation [21, 8]. The resulting soft gloss distribution is injected into the flow memory through a delayed plan-to-flow curriculum. This lets the flow heads first learn stable motion dynamics and then gradually incorporate gloss-level guidance. We further use weaker post-motion CTC and landmark-based gloss losses, $\mathcal{L}_{\text{post}}$ and \mathcal{L}_{lm} , as auxiliary regularizers for lexical organization. The full objective is

$$\mathcal{L}_{\text{signavox}} = \mathcal{L}_{\text{FM}} + \lambda_{\text{bdry}} \mathcal{L}_{\text{bdry}} + \lambda_{\text{plan}} \mathcal{L}_{\text{plan}} + \lambda_{\text{post}} \mathcal{L}_{\text{post}} + \lambda_{\text{lm}} \mathcal{L}_{\text{lm}}. \quad (6)$$

Inference. At inference time, SIGNAVOX is conditioned only on the prior signing context and target role prompt, (H_t, r_t) , and generates the response autoregressively as motion blocks. For each block ℓ , the decoder produces C_ℓ , the boundary head predicts b_ℓ , and the gloss planner predicts an internal soft plan P_ℓ^{plan} . The flow heads are conditioned on $\tilde{C}_\ell = C_\ell + e_{\text{bdry}}(b_\ell) + \alpha \phi(P_\ell^{\text{plan}})$, where α is the final plan-to-flow weight. The gloss plan is therefore an internal prediction, rather than an externally supplied generation input.

Table 2: Quantitative comparison of gloss-level and sentence-level co-articulation generation results. For methods with $r = 4$, four co-articulation frames are predicted. Lower is better for all metrics, while Length Ratio is better when closer to 1.

		DTW-MPJPE ↓			DTW-MPVPE ↓				DTW	DTW	Length
		Body	Hands	Overall	Body	Hands	Face	Overall	PA-MPJPE ↓	PA-MPVPE ↓	Ratio
Gloss	Linear ($r = 4$)	0.0460	0.1841	0.0816	0.0358	0.0231	0.0018	0.0538	0.0769	0.0543	5.3693
	SignConnector [97]	0.0461	0.1843	0.0817	0.0359	0.0231	0.0018	0.0539	0.0770	0.0544	5.0981
	SignD2C ($r = 4$) [75]	0.0466	0.1827	0.0819	0.0368	0.0233	0.0018	0.0559	0.0766	0.0542	5.3693
	BRAID (Ours)	0.0376	0.1384	0.0653	0.0309	0.0171	0.0017	0.0439	0.0610	0.0427	1.2786
Sentence	Linear ($r = 4$)	0.0504	0.2053	0.1020	0.0537	0.0494	0.0243	0.0706	0.0898	0.0651	1.6290
	SignConnector [97]	0.0508	0.2074	0.1028	0.0496	0.0246	0.0227	0.0711	0.0906	0.0657	1.5339
	SignD2C ($r = 4$) [75]	0.0515	0.2055	0.1028	0.0504	0.0246	0.0226	0.0728	0.0900	0.0655	1.6290
	BRAID (Ours)	0.0422	0.1686	0.0757	0.0336	0.0190	0.0015	0.0498	0.0758	0.0507	1.0203

5 Experiments

5.1 Isolated to Continuous Signing

Setup. For gloss-level evaluation, we train the model on 78,316 samples and evaluate it on 8,274 test samples. For sentence-level evaluation, we use 1,526 sentence sequences. We compare our method with a simple linear interpolation baseline and representative sign transition baselines [97, 75]. For a controlled comparison, both the linear interpolation baseline and SignD2C [75] generate only four transition frames at each gloss boundary. At the sentence-level, their gloss-pair outputs are stitched using the same procedure as ours, without the sentence-level duration predictor $\mathcal{D}_{\text{sent}}$.

Evaluation Metrics. For quantitative evaluation, we follow previous works [89, 82] and apply dynamic time splitting (DTW) before computing pose and mesh errors. We report MPJPE/MPVPE and PA-MPJPE/PA-MPVPE, where Procrustes alignment accounts for global pose, scale, and signer-shape differences. Since DTW can absorb duration mismatches, we also report length ratio for sequence-length accuracy.

Results. Table 2 shows that *BRAID* achieves the best overall performance. It consistently reduces DTW-based motion errors over the baselines, indicating that boundary-aware refinement improves co-articulatory motion beyond simple local interpolation. Its length ratio is also closer to 1, suggesting better temporal-scale preservation. Fig. 5 shows that *BRAID* generates more natural co-articulatory transitions than the baselines. Since linear interpolation simply connects the boundary poses of adjacent glosses, large pose discrepancies often produce unnatural articulation and static intermediate poses. SignD2C also generates short transition frames, but it tends to rely strongly on boundary anchors, pulling the motion toward the anchor poses. SignConnector is further limited to interpolating a short connector segment between adjacent signs, which restricts its ability to model broader transition dynamics. In contrast, *BRAID* performs non-rigid boundary refinement after duration-aware resampling, softly adjusting frames around the boundary rather than treating anchors as hard constraints. This enables *BRAID* to synthesize plausible intermediate articulation continuous motion closer to the ground truth.

Ablation Study. As shown in Table 3, performance improves progressively from the raw input to the single-stage variants and further to the full pipeline. This suggests that articulation-frame selection provides cleaner inputs for *BRAID*, with motion-based selection and VideoLLM refinement playing complementary roles.

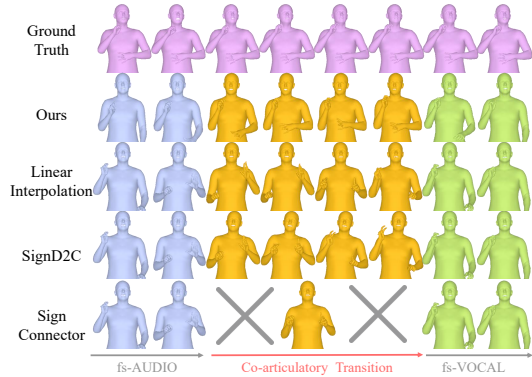


Figure 5: Qualitative results of *BRAID*. We visualize the synthesized motions between two isolated glosses, "fs-AUDIO" (blue) and "fs-VOCAL" (green). The 'X' marks denote the absence of intermediate frames in the transition sequence.

Table 3: Ablation on articulation-frame selection. "G" and "S" denote gloss-pair and sentence levels, respectively.

	DTW-MPJPE ↓		DTW-MPVPE ↓	
	G	S	G	S
Raw	0.0704	0.0790	0.0478	0.0526
Motion-only	0.0693	0.0783	0.0472	0.0523
VideoLLM-only	0.0689	0.0784	0.0471	0.0524
Motion + VideoLLM	0.0653	0.0738	0.0439	0.0486

Table 4: Quantitative results of spoken-language-to-gloss translation. We set $N = 100$ following previous work [91].

	BLEU-4	SacreBLEU	chrF	GPT Struct	GPT Semantic
N -shot [91]	0.094	15.583	51.701	3.674	4.308
No guidance	0.021	8.581	42.818	3.289	4.083
Retrieval-only	0.098	16.512	55.176	3.692	4.331
Rerank-only	0.099	16.506	54.912	3.707	4.332
Ours	0.108	17.062	55.645	3.751	4.351

Spoken language	When do you finish work?	What time did my friend arrive?
GT	IX-2p FINISH WORK WHEN IX-2p	ATTENTION-WAVE POSS-1p FRIEND ARRIVE TIME
N -Shot	WHEN YOU FINISH WORK	TIME WHAT FRIEND POSS-1p ARRIVE
Ours	IX-2p FINISH WORK WHEN	POSS-1p FRIEND ARRIVE TIME WHAT

Figure 6: Qualitative examples of spoken-language-to-gloss translation. Blue omitted reference glosses, and red marks erroneous generated glosses.

Table 5 further ablates the main components of *BRAID*. At the gloss-pair level, removing boundary inpainting or gloss-level duration prediction degrades reconstruction accuracy, confirming the need for boundary-focused refinement and duration-aware resampling. At the sentence level, removing sentence-level duration prediction causes large length mismatch, and hard stitching increases motion error, showing that duration planning and smooth stitching are necessary for temporally aligned continuous sign motion.

Table 5: Ablation study on duration prediction and boundary inpainting.

	DTW MPJPE↓	DTW MPVPE↓	Length Ratio
Training (Gloss-level)			
w/o inpaint	0.0670	0.0881	1.2786
w/o $\mathcal{D}_{\text{gloss}}$	0.0701	0.0480	1.5050
Ours	0.0653	0.0439	1.2786
Stitching (Sentence-level)			
w/o $\mathcal{D}_{\text{sent}}$	0.0863	0.6000	0.4735
Hard Stitching	0.0745	0.0491	1.0203
Ours	0.0738	0.0486	1.0203

5.2 Spoken Language to Gloss

Evaluation Metrics. We evaluate gloss translation using standard translation metrics [56, 59, 58] and GPT-5.2-based evaluation [54]. To complement overlap-based metrics, GPT-5.2 assesses semantic preservation and structural well-formedness. The evaluation prompt is provided in Appendix J.

Results. Table 4 shows that our translator outperforms the previous approach [91] across all metrics. Ablations confirm the importance of guidance, with retrieval and reranking providing complementary gains. As shown in Fig. 17, our translator better follows ASL-style structure, including dataset-style indices and appropriate WH placement. Some dataset-specific meta glosses, such as ATTENTION-WAVE, encode visual or discourse cues unavailable from text alone, which can lower n-gram scores despite reasonable outputs. More results are provided in Appendix I.3.

5.3 Sign Language Conversation

Evaluation Metrics. To evaluate our model, we compare generated response motions with the corresponding ground-truth responses using DTW-MPJPE and DTW-MPVPE. We additionally report Fréchet Gesture Distance (FGD) [88] for distributional motion quality. For response-level semantic alignment, we propose a retrieval-based semantic evaluation method, detailed in Appendix H.1.

Results. Table 6 compares our model with ReMoS [18], a motion-conditioned response generation baseline, and reports ablation results. SIGNAVOX consistently outperforms ReMoS across motion quality and semantic alignment metrics. The ablations show that each grounding component contributes to response generation: $\alpha_s \phi(P_{\ell}^{\text{plan}})$ links the learned gloss plan to the motion generator, $\mathcal{L}_{\text{plan}}$ supervises pre-motion gloss planning, and $\mathcal{L}_{\text{post}} + \mathcal{L}_{\text{lm}}$ supports semantic consistency. Removing all three components results in the largest BLEU-4 drop, indicating that semantic grounding is important for preserving the intended response semantics.

Table 6: Performance comparison with [18] and ablation studies.

Method	FGD ↓	DTW MPJPE ↓	DTW MPVPE ↓	BLEU-4 ↑
ReMoS [18]	83.281	0.1105	0.0788	0.0919
SIGNAVOX	2.9497	0.0800	0.0550	0.0944
⊥ w/o $\alpha_s \phi(P_{\ell}^{\text{plan}})$	4.5312	0.0821	0.0568	0.0900
⊥ w/o $\mathcal{L}_{\text{plan}}$	2.9683	0.0818	0.0565	0.0850
⊥ w/o $\mathcal{L}_{\text{post}} + \mathcal{L}_{\text{lm}}$	4.1140	0.0868	0.0565	0.0720
⊥ w/o semantic grounding	8.2454	0.0810	0.0565	0.0520

6 Conclusion

We introduce a sign-centered approach for constructing and modeling continuous sign language motion. We introduced SIGNAVOX-W and SIGNAVOX-U as 3D signing resources, proposed *BRAID* for co-articulation-aware composition of isolated signs, and further developed SIGNAVOX, a sign-to-sign conversational model for generating continuous 3D sign responses. Together, these components establish an initial step toward direct sign-centered conversational modeling. Additional discussion on limitations and future work is provided in the Appendix A.

Acknowledgments and Disclosure of Funding

This work was supported in part by the IITP RS-2024-00457882 (AI Research Hub Project), IITP 2020-II201361, NRF RS-2024-00345806, NRF RS-2023-002620, NRF-2024S1A5C3A03046579, and RQT-25-120390. Affiliations: Department of Artificial Intelligence (Y.K, J.K, S.J.H), Department of Computer Science (K.C, M.K).

References

- [1] Samuel Albanie, Gül Varol, Liliane Momeni, Triantafyllos Afouras, Joon Son Chung, Neil Fox, and Andrew Zisserman. Bsl-1k: Scaling up co-articulated sign language recognition using mouthing cues. In *European conference on computer vision*, pages 35–53. Springer, 2020.
- [2] Vassilis Athitsos, Carol Neidle, Stan Sclaroff, Joan Nash, Alexandra Stefan, Quan Yuan, and Ashwin Thangali. The american sign language lexicon video dataset. In *2008 IEEE computer society conference on computer vision and pattern recognition workshops*, pages 1–8. IEEE, 2008.
- [3] Shuai Bai, Yuxuan Cai, Ruizhe Chen, Keqin Chen, Xionghui Chen, Zesen Cheng, Lianghao Deng, Wei Ding, Chang Gao, Chunjiang Ge, et al. Qwen3-vl technical report. *arXiv preprint arXiv:2511.21631*, 2025.
- [4] Lauren Berger, Jennie Pyers, Amy Lieberman, and Naomi Caselli. Parent american sign language skills correlate with child—but not toddler—asl vocabulary size. *Language Acquisition*, 31(2):85–99, 2024.
- [5] Danielle Bragg, Oscar Koller, Mary Bellard, Larwan Berke, Patrick Boudreault, Annelies Braffort, Naomi Caselli, Matt Huenerfauth, Hernisa Kacorri, Tessa Verhoef, et al. Sign language recognition, generation, and translation: An interdisciplinary perspective. In *Proceedings of the 21st international ACM SIGACCESS conference on computers and accessibility*, pages 16–31, 2019.
- [6] Zhongang Cai, Wanqi Yin, Ailing Zeng, Chen Wei, Qingping Sun, Wang Yanjun, Hui En Pang, Haiyi Mei, Mingyuan Zhang, Lei Zhang, Chen Change Loy, Lei Yang, and Ziwei Liu. SMPLer-X: Scaling up expressive human pose and shape estimation. In *Advances in Neural Information Processing Systems*, 2023.
- [7] Necati Cihan Camgoz, Simon Hadfield, Oscar Koller, Hermann Ney, and Richard Bowden. Neural sign language translation. In *Proceedings of the IEEE conference on computer vision and pattern recognition*, pages 7784–7793, 2018.
- [8] Necati Cihan Camgoz, Oscar Koller, Simon Hadfield, and Richard Bowden. Sign language transformers: Joint end-to-end sign language recognition and translation. In *Proceedings of the IEEE/CVF conference on computer vision and pattern recognition*, pages 10023–10033, 2020.
- [9] Naomi K Caselli, Zed Sevcikova Sehyr, Ariel M Cohen-Goldberg, and Karen Emmorey. Asl-lex: A lexical database of american sign language. *Behavior research methods*, 49(2):784–801, 2017.
- [10] Yutong Chen, Ronglai Zuo, Fangyun Wei, Yu Wu, Shujie Liu, and Brian Mak. Two-stream network for sign language recognition and translation. *Advances in Neural Information Processing Systems*, 35: 17043–17056, 2022.
- [11] Amanda Duarte, Shruti Palaskar, Lucas Ventura, Deepti Ghadiyaram, Kenneth DeHaan, Florian Metze, Jordi Torres, and Xavier Giro-i Nieto. How2sign: a large-scale multimodal dataset for continuous american sign language. In *Proceedings of the IEEE/CVF conference on computer vision and pattern recognition*, pages 2735–2744, 2021.
- [12] Hugging Face. Everyday conversations for llms. <https://huggingface.co/datasets/HuggingFaceTB/everyday-conversations-llama3.1-2k>, 2024.
- [13] Sen Fang, Chen Chen, Lei Wang, Ce Zheng, Chunyu Sui, and Yapeng Tian. Signllm: Sign language production large language models. In *Proceedings of the IEEE/CVF International Conference on Computer Vision*, pages 6622–6634, 2025.
- [14] Panagiotis P Filintisis, George Retsinas, Foivos Paraperas-Papantoniou, Athanasios Katsamanis, Anastasios Roussos, and Petros Maragos. Spectre: Visual speech-informed perceptual 3d facial expression reconstruction from videos. In *Proceedings of the IEEE/CVF conference on computer vision and pattern recognition*, pages 5745–5755, 2023.
- [15] Thibault Formal, Benjamin Piwowarski, and Stéphane Clinchant. Splade: Sparse lexical and expansion model for first stage ranking. In *Proceedings of the 44th International ACM SIGIR Conference on Research and Development in Information Retrieval*, pages 2288–2292, 2021.

- [16] Jens Forster, Christoph Schmidt, Thomas Hoyoux, Oscar Koller, Uwe Zelle, Justus H Piater, and Hermann Ney. Rwth-phoenix-weather: A large vocabulary sign language recognition and translation corpus. In *LREC*, volume 9, pages 3785–3789, 2012.
- [17] Jens Forster, Christoph Schmidt, Oscar Koller, Martin Bellgardt, and Hermann Ney. Extensions of the sign language recognition and translation corpus rwth-phoenix-weather. In *LREC*, pages 1911–1916, 2014.
- [18] Anindita Ghosh, Rishabh Dabral, Vladislav Golyanik, Christian Theobalt, and Philipp Slusallek. Remos: 3d motion-conditioned reaction synthesis for two-person interactions. In *European conference on computer vision*, pages 418–437. Springer, 2024.
- [19] Jia Gong, Lin Geng Foo, Yixuan He, Hossein Rahmani, and Jun Liu. Llms are good sign language translators. In *Proceedings of the IEEE/CVF conference on computer vision and pattern recognition*, pages 18362–18372, 2024.
- [20] Corina Goodwin and Diane Lillo-Martin. Deaf and hearing american sign language–english bilinguals: Typical bilingual language development. *Journal of Deaf Studies and Deaf Education*, 28(4):350–362, 2023.
- [21] Alex Graves, Santiago Fernández, Faustino Gomez, and Jürgen Schmidhuber. Connectionist temporal classification: labelling unsegmented sequence data with recurrent neural networks. In *Proceedings of the 23rd international conference on Machine learning*, pages 369–376, 2006.
- [22] Jianyuan Guo, Peike Li, and Trevor Cohn. Bridging sign and spoken languages: Pseudo gloss generation for sign language translation. In *The Thirty-ninth Annual Conference on Neural Information Processing Systems*.
- [23] Wyatt C Hall. What you don’t know can hurt you: The risk of language deprivation by impairing sign language development in deaf children. *Maternal and child health journal*, 21(5):961–965, 2017.
- [24] Tiankai Hang, Shuyang Gu, Chen Li, Jianmin Bao, Dong Chen, Han Hu, Xin Geng, and Baining Guo. Efficient diffusion training via min-snr weighting strategy. In *Proceedings of the IEEE/CVF international conference on computer vision*, pages 7441–7451, 2023.
- [25] Marlene Hilzensauer and Klaudia Krammer. A multilingual dictionary for sign languages: "spreadthesign". In *ICER2015 Proceedings*, pages 7826–7834. IATED, 2015. URL <https://spreadthesign.com>.
- [26] Jonathan Ho, Ajay Jain, and Pieter Abbeel. Denoising diffusion probabilistic models. *Advances in neural information processing systems*, 33:6840–6851, 2020.
- [27] Julie Hochgesang, OA Crasborn, and Diane Lillo-Martin. Building the asl signbank. lemmatization principles for asl. 2018. doi: 10.6084/m9.figshare.9741788. URL <http://aslsignbank.haskins.yale.edu>.
- [28] Matthew Honnibal, Ines Montani, Sofie Van Landeghem, and Adriane Boyd. spaCy: Industrial-strength natural language processing in python, 2020. URL <https://doi.org/10.5281/zenodo.1212303>.
- [29] Glenn Jocher, Jing Qiu, and Ayush Chaurasia. Ultralytics YOLO, January 2023. URL <https://github.com/ultralytics/ultralytics>.
- [30] Youngmin Kim and Hyeongbo Baek. Preprocessing for keypoint-based sign language translation without glosses. *Sensors*, 23(6):3231, 2023.
- [31] Youngmin Kim, Jiwan Chung, Jisoo Kim, Sunghyun Lee, Sangkyu Lee, Junhyeok Kim, Cheoljong Yang, and Youngjae Yu. Speaking beyond language: A large-scale multimodal dataset for learning nonverbal cues from video-grounded dialogues. In *Proceedings of the 63rd Annual Meeting*, pages 2247–2265, Vienna, Austria, July 2025. Association for Computational Linguistics. ISBN 979-8-89176-251-0.
- [32] Sang-Ki Ko, Chang Jo Kim, Hyedong Jung, and Choongsang Cho. Neural sign language translation based on human keypoint estimation. *Applied sciences*, 9(13):2683, 2019.
- [33] Roger Koenker and Gilbert Bassett Jr. Regression quantiles. *Econometrica: journal of the Econometric Society*, pages 33–50, 1978.
- [34] Amy R Lederberg, Brenda Schick, and Patricia E Spencer. Language and literacy development of deaf and hard-of-hearing children: successes and challenges. *Developmental psychology*, 49(1):15, 2013.
- [35] Amy R Lederberg, Elizabeth M Miller, Susan R Easterbrooks, and Carol McDonald Connor. Foundations for literacy: An early literacy intervention for deaf and hard-of-hearing children. *Journal of deaf studies and deaf education*, 19(4):438–455, 2014.

- [36] Dong-Ho Lee, Adyasha Maharana, Jay Pujara, Xiang Ren, and Francesco Barbieri. Realtalk: A 21-day real-world dataset for long-term conversation. *arXiv preprint arXiv:2502.13270*, 2025.
- [37] Yeonkyung Lee, Dayun Ju, Youngmin Kim, Seil Kang, and Seong Jae Hwang. Vikey: Enhancing temporal understanding in videos via visual prompting. *arXiv preprint arXiv:2603.23186*, 2026.
- [38] Patrick Lewis, Ethan Perez, Aleksandra Piktus, Fabio Petroni, Vladimir Karpukhin, Naman Goyal, Heinrich Küttler, Mike Lewis, Wen-tau Yih, Tim Rocktäschel, et al. Retrieval-augmented generation for knowledge-intensive nlp tasks. *Advances in neural information processing systems*, 33:9459–9474, 2020.
- [39] Dongxu Li, Cristian Rodriguez, Xin Yu, and Hongdong Li. Word-level deep sign language recognition from video: A new large-scale dataset and methods comparison. In *Proceedings of the IEEE/CVF winter conference on applications of computer vision*, pages 1459–1469, 2020.
- [40] Tianhong Li, Yonglong Tian, He Li, Mingyang Deng, and Kaiming He. Autoregressive image generation without vector quantization. *Advances in Neural Information Processing Systems*, 37:56424–56445, 2024.
- [41] Tianye Li, Timo Bolkart, Michael J Black, Hao Li, and Javier Romero. Learning a model of facial shape and expression from 4d scans. *ACM Trans. Graph.*, 36(6):194–1, 2017.
- [42] Yanran Li, Hui Su, Xiaoyu Shen, Wenjie Li, Ziqiang Cao, and Shuzi Niu. Dailydialog: A manually labelled multi-turn dialogue dataset. In *Proceedings of the Eighth International Joint Conference on Natural Language Processing (Volume 1: Long Papers)*, pages 986–995, 2017.
- [43] Zecheng Li, Wengang Zhou, Weichao Zhao, Kepeng Wu, Hezhen Hu, and Houqiang Li. Uni-sign: Toward unified sign language understanding at scale. *arXiv preprint arXiv:2501.15187*, 2025.
- [44] Kezhou Lin, Xiaohan Wang, Linchao Zhu, Ke Sun, Bang Zhang, and Yi Yang. Gloss-free end-to-end sign language translation. In *Proceedings of the 61st Annual Meeting of the Association for Computational Linguistics (Volume 1: Long Papers)*, pages 12904–12916, 2023.
- [45] Yaron Lipman, Ricky TQ Chen, Heli Ben-Hamu, Maximilian Nickel, and Matthew Le. Flow matching for generative modeling. In *The Eleventh International Conference on Learning Representations*.
- [46] Ross E Mitchell and Michael A Karchmer. Chasing the mythical ten percent: Parental hearing status of deaf and hard of hearing students in the united states. *Sign language studies*, 4(2):138–163, 2004.
- [47] Liliane Momeni, Hannah Bull, KR Prajwal, Samuel Albanie, Gül Varol, and Andrew Zisserman. Automatic dense annotation of large-vocabulary sign language videos. In *European Conference on Computer Vision*, pages 671–690. Springer, 2022.
- [48] Jill P Morford, Erin Wilkinson, Agnes Villwock, Pilar Piñar, and Judith F Kroll. When deaf signers read english: Do written words activate their sign translations? *Cognition*, 118(2):286–292, 2011.
- [49] Jill P Morford, Judith F Kroll, Pilar Piñar, and Erin Wilkinson. Bilingual word recognition in deaf and hearing signers: Effects of proficiency and language dominance on cross-language activation. *Second Language Research*, 30(2):251–271, 2014.
- [50] Meinard Müller. *Information retrieval for music and motion*. Springer, 2007.
- [51] Carol Neidle. A user’s guide to signstream® 3. *Boston, MA: American Sign Language Linguistic Research Project Report*, (16), 2017.
- [52] Carol Neidle, Augustine Opoku, and Dimitris Metaxas. Asl video corpora & sign bank: Resources available through the american sign language linguistic research project (asllrp). *arXiv preprint arXiv:2201.07899*, 2022.
- [53] OpenAI. Hello gpt-4o. <https://openai.com/index/hello-gpt-4o/>, 2024. Accessed: 2026-04-22.
- [54] OpenAI. Introducing gpt-5.2, 2025. URL <https://openai.com/index/introducing-gpt-5-2/>. Accessed: 2026-03-24.
- [55] Carol A Padden and Tom L Humphries. *Deaf in America: Voices from a culture*. Harvard University Press, 1988.
- [56] Kishore Papineni, Salim Roukos, Todd Ward, and Wei-Jing Zhu. Bleu: a method for automatic evaluation of machine translation. In *Proceedings of the 40th annual meeting of the Association for Computational Linguistics*, pages 311–318, 2002.

- [57] Georgios Pavlakos, Vasileios Choutas, Nima Ghorbani, Timo Bolkart, Ahmed AA Osman, Dimitrios Tzionas, and Michael J Black. Expressive body capture: 3d hands, face, and body from a single image. In *Proceedings of the IEEE/CVF conference on computer vision and pattern recognition*, pages 10975–10985, 2019.
- [58] Maja Popović. chrF: character n-gram f-score for automatic mt evaluation. In *Proceedings of the tenth workshop on statistical machine translation*, pages 392–395, 2015.
- [59] Matt Post. A call for clarity in reporting bleu scores. In *Proceedings of the third conference on machine translation: Research papers*, pages 186–191, 2018.
- [60] Joseph Redmon and Ali Farhadi. Yolov3: An incremental improvement. *arXiv preprint arXiv:1804.02767*, 2018.
- [61] Stephen Robertson and Hugo Zaragoza. *The probabilistic relevance framework: BM25 and beyond*, volume 4. Now Publishers Inc, 2009.
- [62] J. Romero, Dimitrios Tzionas, and Michael J. Black. Embodied hands. In *ACM Transactions on Graphics*, 2017. doi: 10.1145/3130800.3130883.
- [63] Ben Saunders, Necati Cihan Camgoz, and Richard Bowden. Progressive transformers for end-to-end sign language production. In *European Conference on Computer Vision*, pages 687–705. Springer, 2020.
- [64] Ben Saunders, Necati Cihan Camgoz, and Richard Bowden. Continuous 3d multi-channel sign language production via progressive transformers and mixture density networks. *International journal of computer vision*, 129(7):2113–2135, 2021.
- [65] Ben Saunders, Necati Cihan Camgoz, and Richard Bowden. Signing at scale: Learning to co-articulate signs for large-scale photo-realistic sign language production. In *Proceedings of the IEEE/CVF Conference on Computer Vision and Pattern Recognition*, pages 5141–5151, 2022.
- [66] Abraham Savitzky and Marcel JE Golay. Smoothing and differentiation of data by simplified least squares procedures. *Analytical chemistry*, 36(8):1627–1639, 1964.
- [67] Signing Savvy. Signing savvy: ASL sign language video dictionary, 2026. URL <https://www.signingsavvy.com>. Accessed: 2026-02-05.
- [68] Bowen Shi, Diane Brentari, Gregory Shakhnarovich, and Karen Livescu. Open-domain sign language translation learned from online video. In *Proceedings of the 2022 Conference on Empirical Methods in Natural Language Processing*, pages 6365–6379, 2022.
- [69] Aleksandar Shtedritski, Christian Rupprecht, and Andrea Vedaldi. What does clip know about a red circle? visual prompt engineering for vlms. In *Proceedings of the IEEE/CVF International Conference on Computer Vision*, pages 11987–11997, 2023.
- [70] Sign ASL. Sign ASL: An American Sign Language Dictionary. <https://www.signasl.org/>, 2026. Accessed: 2026-03-01.
- [71] Jiaming Song, Chenlin Meng, and Stefano Ermon. Denoising diffusion implicit models. *arXiv preprint arXiv:2010.02502*, 2020.
- [72] William C Stokoe. Sign language structure. *Annual review of anthropology*, pages 365–390, 1980.
- [73] Stephanie Stoll, Necati Cihan Camgöz, Simon Hadfield, and Richard Bowden. Sign language production using neural machine translation and generative adversarial networks. In *Proceedings of the 29th British Machine Vision Conference (BMVC 2018)*. British Machine Vision Association, 2018.
- [74] Jianlin Su, Murtadha Ahmed, Yu Lu, Shengfeng Pan, Wen Bo, and Yunfeng Liu. Roformer: Enhanced transformer with rotary position embedding. *Neurocomputing*, 568:127063, 2024.
- [75] Shengeng Tang, Jiayi He, Lechao Cheng, Jingjing Wu, Dan Guo, and Richang Hong. Discrete to continuous: Generating smooth transition poses from sign language observations. In *Proceedings of the Computer Vision and Pattern Recognition Conference*, pages 3481–3491, 2025.
- [76] Garrett Tanzer and Biao Zhang. Youtube-sl-25: A large-scale, open-domain multilingual sign language parallel corpus. *arXiv preprint arXiv:2407.11144*, 2024.
- [77] Guy Tevet, Sigal Raab, Brian Gordon, Yonatan Shafir, Daniel Cohen-Or, and Amit H Bermano. Human motion diffusion model. *arXiv preprint arXiv:2209.14916*, 2022.

- [78] Alexander Tong, Kilian Fatras, Nikolay Malkin, Guillaume Hugué, Yanlei Zhang, Jarrid Rector-Brooks, Guy Wolf, and Yoshua Bengio. Improving and generalizing flow-based generative models with minibatch optimal transport. *arXiv preprint arXiv:2302.00482*, 2023.
- [79] Dave Uthus, Garrett Tanzer, and Manfred Georg. Youtube-asl: A large-scale, open-domain american sign language-english parallel corpus. *Advances in Neural Information Processing Systems*, 36:29029–29047, 2023.
- [80] Hamid Vaezi Joze and Oscar Koller. Ms-asl: A large-scale data set and benchmark for understanding american sign language. In *The British Machine Vision Conference (BMVC)*, September 2019.
- [81] Gul Varol, Liliane Momeni, Samuel Albanie, Triantafyllos Afouras, and Andrew Zisserman. Read and attend: Temporal localisation in sign language videos. In *Proceedings of the IEEE/CVF Conference on Computer Vision and Pattern Recognition*, pages 16857–16866, 2021.
- [82] Harry Walsh, Ed Fish, Ozge Mercanoglu Sincan, Mohamed Ilyes Lakhel, Richard Bowden, Neil Fox, Bencie Woll, Kepeng Wu, Zecheng Li, Weichao Zhao, et al. Slrtp2025 sign language production challenge: Methodology, results and future work. In *Proceedings of the IEEE/CVF Conference on Computer Vision and Pattern Recognition*, pages 4148–4158, 2025.
- [83] Ryan Wong, Necati Cihan Camgoz, and Richard Bowden. Sign2gpt: Leveraging large language models for gloss-free sign language translation. *arXiv preprint arXiv:2405.04164*, 2024.
- [84] Yongliang Wu, Xinting Hu, Yuyang Sun, Yizhou Zhou, Wenbo Zhu, Fengyun Rao, Bernt Schiele, and Xu Yang. Number it: Temporal grounding videos like flipping manga. In *Proceedings of the Computer Vision and Pattern Recognition Conference*, pages 13754–13765, 2025.
- [85] Shitao Xiao, Zheng Liu, Peitian Zhang, Niklas Muennighoff, Defu Lian, and Jian-Yun Nie. C-pack: Packed resources for general chinese embeddings. In *Proceedings of the 47th international ACM SIGIR conference on research and development in information retrieval*, pages 641–649, 2024.
- [86] Pan Xie, Qipeng Zhang, Peng Taiying, Hao Tang, Yao Du, and Zexian Li. G2p-ddm: Generating sign pose sequence from gloss sequence with discrete diffusion model. In *Proceedings of the AAAI Conference on Artificial Intelligence*, volume 38, pages 6234–6242, 2024.
- [87] Kayo Yin and Jesse Read. Better sign language translation with stmc-transformer. In *Proceedings of the 28th International Conference on Computational Linguistics*, pages 5975–5989, 2020.
- [88] Youngwoo Yoon, Bok Cha, Joo-Haeng Lee, Minsu Jang, Jaeyeon Lee, Jaehong Kim, and Geehyuk Lee. Speech gesture generation from the trimodal context of text, audio, and speaker identity. *ACM Transactions on Graphics (TOG)*, 39(6):1–16, 2020.
- [89] Zhengdi Yu, Shaoli Huang, Yongkang Cheng, and Tolga Birdal. Signavatars: A large-scale 3d sign language holistic motion dataset and benchmark. In *European Conference on Computer Vision*, pages 1–19. Springer, 2024.
- [90] Zhengdi Yu, Stefanos Zafeiriou, and Tolga Birdal. Dyn-hamr: Recovering 4d interacting hand motion from a dynamic camera. In *Proceedings of the Computer Vision and Pattern Recognition Conference*, pages 27716–27726, 2025.
- [91] Han Zhang, Rotem Shalev-Arkushin, Vasileios Baltatzis, Connor Gillis, Gierad Laput, Raja Kushalnagar, Lorna C Quandt, Leah Findlater, Abdelkareem Bedri, and Colin Lea. Towards ai-driven sign language generation with non-manual markers. In *Proceedings of the 2025 CHI Conference on Human Factors in Computing Systems*, pages 1–26, 2025.
- [92] Sen Zhang, Xiaoxiao He, Di Liu, Zhaoyang Xia, Mingyu Zhao, Chaowei Tan, Vivian Li, Bo Liu, Dimitris N Metaxas, and Mubbasir Kapadia. Large sign language models: Toward 3d american sign language translation. *arXiv preprint arXiv:2511.08535*, 2025.
- [93] Benjia Zhou, Zhigang Chen, Albert Clapés, Jun Wan, Yanyan Liang, Sergio Escalera, Zhen Lei, and Du Zhang. Gloss-free sign language translation: Improving from visual-language pretraining. In *Proceedings of the IEEE/CVF International Conference on Computer Vision*, pages 20871–20881, 2023.
- [94] Hao Zhou, Wengang Zhou, Yun Zhou, and Houqiang Li. Spatial-temporal multi-cue network for continuous sign language recognition. In *Proceedings of the AAAI conference on artificial intelligence*, volume 34, pages 13009–13016, 2020.

- [95] Hao Zhou, Wengang Zhou, Weizhen Qi, Junfu Pu, and Houqiang Li. Improving sign language translation with monolingual data by sign back-translation. In *Proceedings of the IEEE/CVF conference on computer vision and pattern recognition*, pages 1316–1325, 2021.
- [96] Kaiyang Zhou, Yongxin Yang, Andrea Cavallaro, and Tao Xiang. Omni-scale feature learning for person re-identification. In *Proceedings of the IEEE/CVF international conference on computer vision*, pages 3702–3712, 2019.
- [97] Ronglai Zuo, Fangyun Wei, Zenggui Chen, Brian Mak, Jiaolong Yang, and Xin Tong. A simple baseline for spoken language to sign language translation with 3d avatars. In *European Conference on Computer Vision*, pages 36–54. Springer, 2024.

Appendix

A	Limitations & Future Works	18
B	Ethical Consideration	18
C	Key Concepts in Sign Language	18
D	Details of Dataset	19
D.1	Data Analysis	19
D.1.1	Statistics	19
D.1.2	Data Distribution of Conversational Glosses	19
D.2	Details of 3D Representation	20
D.3	Data Quality Control	21
D.4	Data Visualization	22
D.5	SIGNAVOX Annotation	22
D.6	Licensing	23
E	Details of Frame Selection	25
E.1	Energy-Based Preparation and Retraction Trimming	25
E.2	Posture Cue and Hyperparameters	26
F	Details of Isolated to Continuous	26
F.1	Details of Data Setup.	26
F.2	Consistency Analysis	27
F.3	Duration Predictor	28
F.4	Details of <i>BRAID</i>	29
F.5	Inference-Time Composition	30
G	Details of Spoken Language to Gloss	31
G.1	Hyperparameters	31
G.2	Experimental Details	31
H	Details of Sign Language Conversational Model	31
H.1	Retrieval-Based Semantic Evaluation	31
H.2	Implementation Details	32
H.3	Loss Definitions	33
I	Additional Experiments Results	34
I.1	Frame Selection	34
I.2	Isolated-to-Continuous Signing	35
I.3	Spoken Language to Gloss	36
I.4	Sign-to-Sign Conversation	36
I.4.1	Retrieval-Based Semantic Evaluation Method	36

I.4.2	Qualitative Results	37
J	LLM Prompt	38
J.1	VideoLLM Prompt for Articulation Frame Selection	38
J.2	GPT Evaluation Prompt for Spoken to Gloss Translation	38
J.3	Spoken to Gloss Translation System Prompt	38

A Limitations & Future Works

While our framework provides a step toward sign-centered generation and interaction, several limitations remain. First, our dataset and models rely on 3D motion features extracted by existing body, hand, and face reconstruction models. As a result, the quality of the resulting motion representation is bounded by the accuracy of these estimators, particularly in challenging cases such as occlusion, fast hand motion, or low-resolution videos. Improving sign-specific 3D reconstruction remains an important direction for future work.

Second, although our representation includes facial parameters and captures limited non-manual signals, it does not fully cover the rich non-manual components of sign language, including gaze, head movement, eyebrow motion, mouthing, and other grammatical or affective cues. Future work should incorporate more expressive representations and explicit modeling of non-manual signals to better capture the linguistic structure of signing.

Third, our spoken-language-to-gloss conversion follows SignStream-style annotation conventions. This provides a consistent rule set for constructing gloss sequences, but also limits the framework to a particular glossing style. Extending the pipeline to accommodate different annotation conventions, glossing style. Extending the pipeline to accommodate different annotation conventions, sign languages, and community-specific variation is an important future direction.

Finally, evaluating generated sign conversations remains challenging. Our evaluation protocol provides useful proxies for motion quality and semantic recoverability, but it cannot fully measure linguistic correctness, non-manual expression, discourse-level coherence, or human-perceived naturalness. More comprehensive evaluation with expert signers and members of the signing community will be necessary for future sign-centered conversational systems.

B Ethical Consideration

Our dataset is constructed from publicly accessible sign language videos collected from the web. Since these materials contain identifiable human subjects, we carefully considered privacy, consent, and redistribution issues throughout the dataset construction process. First, we do not redistribute the original raw videos as part of the released dataset. Instead, whenever possible, we provide only links or references to the original source pages, so that access to the underlying content remains tied to the original hosting platform. This is intended to reduce unnecessary redistribution of personally identifiable visual data while preserving traceability to the original source. Second, for qualitative examples shown in the paper and appendix, we anonymize the signer by masking the face region. These visual examples are included only to illustrate dataset characteristics and model behavior, and we aim to minimize the exposure of identifiable appearance information in all presented figures. Third, because the dataset is collected from web sources, we acknowledge that public accessibility does not necessarily imply that all forms of downstream reuse carry the same expectation from the original signers. We therefore adopt a conservative release policy that focuses on processed annotations and source references rather than direct redistribution of raw visual content. We additionally emphasize that the dataset is intended for academic research purposes, and any future use should respect the terms, licenses, and access conditions associated with the original sources. Finally, we recognize that web-collected sign language data may reflect biases in source availability, recording conditions, signer demographics, and platform-specific content practices. Such factors may influence both dataset composition and downstream model behavior. We therefore view this dataset as a research resource and encourage its use with appropriate caution, particularly in settings involving human identity, privacy, or real-world deployment.

C Key Concepts in Sign Language

- *Isolated sign.* A single lexical sign produced independently, typically containing handshape, hand motion, body pose, and, when relevant, facial expression.
- *Continuous sign.* A sequence of signs produced as a continuous utterance, where adjacent signs are connected through natural transitions and co-articulation.
- *Co-articulation.* The motion adaptation that occurs around the boundary between adjacent signs, reflecting how neighboring signs influence each other in timing and movement.
- *Gloss.* A written label used to represent a sign, typically following sign language order and reflecting aspects of sign language grammar [72].
- *Articulation.* The core motion segment that realizes the lexical content of a sign, excluding preparation, retraction, or idle frames.
- *Preparation.* The motion before the core articulation, where the signer moves toward the starting configuration of a sign.

Table 7: Statistics of the data sources used to construct the video-gloss dictionary after preprocessing.

	# Videos	# Gloss	Duration (h)	Annotations	Resolution	# Frames (Min, Max, Mean)
Signbank [27]	3,402	2,836	2.34	Gloss, Synonym	Various	33 / 381 / 76.12
SignASL [70]	35,833	28,269	34.40	Gloss	Various	16 / 457 / 101.50
Spreadthesign [25]	9,955	9,531	10.24	Gloss, POS	320 × 240	44 / 379 / 100.75
SigningSavvy [67]	13,461	11,493	8.75	Gloss	640 × 360	19 / 322 / 71.43
MS-ASL [80]	17,822	1,000	15.57	Gloss, Synonym	Various	9 / 271 / 89.11
WLASL [39]	11,836	1,992	7.97	Gloss	Various	15 / 233 / 69.11

Table 8: Detailed dataset statistics split by Train, Validation, and Test sets.

Source	# Dialogues			# Turns			# Sentences			# Avg. Frames/Sent		
	Train	Val	Test	Train	Val	Test	Train	Val	Test	Train	Val	Test
Dailydialog [42]	8,776	1,095	1,098	66,279	8,156	8,465	106,154	13,313	13,590	174.4	174.3	172.8
Everyday [12]	1,786	225	225	10,150	1,268	1,276	18,597	2,256	2,257	254.7	260.0	253.1
RealTalk [36]	166	21	21	5,234	833	641	8,471	1,522	1,038	258.9	268.1	284.5
Total	10,728	1,341	1,344	81,663	10,257	10,382	133,222	17,091	16,885	191.8	194.8	191.2

- *Retraction*. The motion after the core articulation, where the signer moves away from the completed sign.
- *Gloss sequence*. An ordered sequence of gloss labels representing a continuous sign utterance. In our system, it serves as an intermediate representation between spoken language and 3D sign motion.
- *Spoken language*. The text sentence associated with a sign utterance. It is not necessarily word-aligned with the gloss sequence, since sign languages and spoken languages can differ in word order and grammatical structure.

D Details of Dataset

D.1 Data Analysis

D.1.1 Statistics

The statistics of the processed source datasets used to construct SIGNAVOX-W are presented in Table 7. As shown in the table, the source datasets vary substantially in scale, annotation type, resolution, and video length. In particular, while SignASL [70] and Spreadthesign [25] provide large vocabularies and broad lexical coverage, other resources such as MS-ASL [80] and WLASL [39] offer complementary samples with different annotation schemes and video characteristics. This diversity allows us to collect lexical sign videos from heterogeneous sources, although it also necessitates careful quality control and normalization.

The statistics of the processed source datasets used to construct SIGNAVOX-U are presented in Table 8. As shown in the table, the source datasets differ in conversational scale, turn structure, sentence count, and resulting motion length. DailyDialog [42] provides the largest number of dialogues and sentences, offering broad coverage of everyday multi-turn interactions, while Everyday Conversations [12] and RealTalk [36] contribute complementary dialogue patterns with longer average sentence-level motion sequences. After spoken-language-to-gloss conversion and isolated-to-continuous construction, SIGNAVOX-U contains 10,728 training dialogues, 81,663 training turns, and 133,222 training sentences, with an average of 191.8 frames per sentence. This scale and diversity allow us to construct a dialogue-style continuous signing dataset suitable for training sign-centered conversational models.

D.1.2 Data Distribution of Conversational Glosses

To examine whether SIGNAVOX-W provides sufficient lexical coverage for daily sign conversation, we analyze the semantic distribution of its gloss-level videos. For each video, we provide the gloss and its meaning label to GPT-4o and assign it to a taxonomy consisting of five high-level conversational groups and 15 fine-grained categories. We then count the video-level gloss instances in each category and visualize the resulting distribution in Fig. 7.

The resulting distribution shows that SIGNAVOX-W covers a broad range of conversational functions rather than being concentrated in a narrow set of signs. The largest portion corresponds to *Description & Attributes* with 30.6%, including qualitative descriptions, physical states, and emotions. This indicates that the

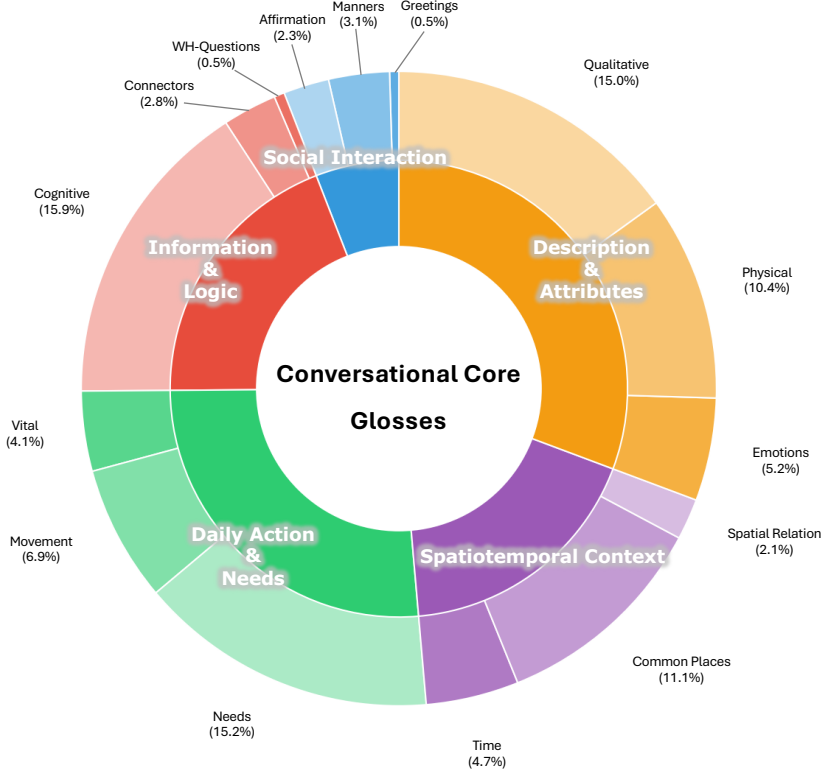


Figure 7: Semantic distribution of gloss-level videos in SIGNAVOX-W.

dataset contains many glosses for describing people, objects, and states, which are essential for generating natural sign responses. *Daily Actions & Needs* accounts for 26.2%, covering movement, vital actions, and requests. These signs directly support daily-life interactions and provide action-oriented expressions required in practical conversations. The dataset also contains substantial coverage of contextual and logical expressions. *Information & Logic* accounts for 19.2%, mainly including cognitive states, connectors, and question-related expressions, while *Spatiotemporal Context* accounts for 17.9%, including time references, common places, and spatial relations. These categories are important for constructing sentence-level sign videos, since they help combine individual glosses into coherent utterances with temporal, spatial, and causal structure. Although *Social Interaction* occupies a smaller portion at 5.9%, this is expected given the nature of this category. Social-interaction glosses, such as greetings, manners, and affirmation or denial, form a comparatively small and closed set of conventional expressions. Once these basic interactional signs are covered, they can be repeatedly reused across different conversational contexts. In contrast, actions, attributes, places, and logical expressions are more open-ended and content-bearing, requiring broader lexical coverage to support diverse sentence construction.

Overall, this distribution suggests that SIGNAVOX-W provides functionally diverse gloss-level building blocks for composing sentence-level sign videos and training a sign-to-sign conversational model.

D.2 Details of 3D Representation

The main 3D motion representation used in our experiments follows Equation 1. For completeness, we also provide an augmented annotation that includes the SMPL-X global body orientation and the FLAME neck rotation in addition to the features in Equation 1. For each frame t , the augmented representation is defined as

$$\Theta_t^{\text{body}} = [\mathbf{r}_t^{\text{body}}, \boldsymbol{\theta}_t^{\text{body}}], \quad \Theta_t^{\text{face}} = [\mathbf{r}_t^{\text{neck}}, \boldsymbol{\theta}_t^{\text{jaw}}, \psi_t], \quad \Theta_t^{\text{hands}} = [\boldsymbol{\theta}_t^{\text{rhand}}, \boldsymbol{\theta}_t^{\text{lhand}}]. \quad (7)$$



Figure 8: Examples of representative cases considered during data quality control.

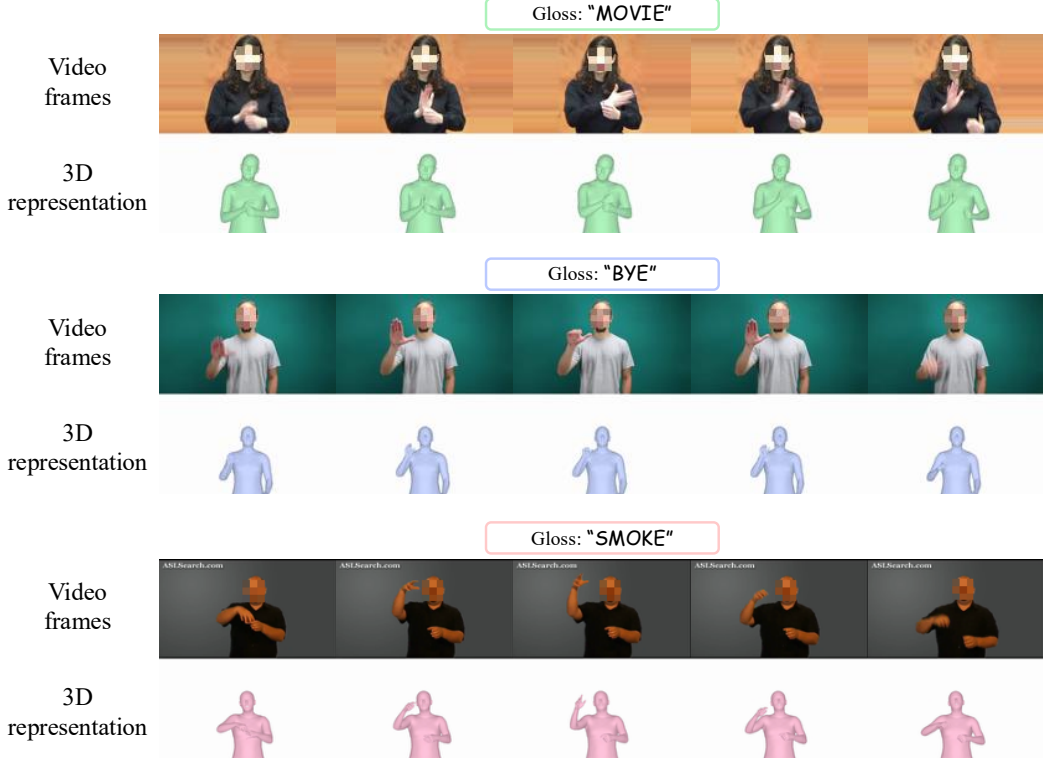


Figure 9: Visualized examples of SIGNAVOX-W.

Here, $\mathbf{r}_t^{\text{body}} \in \mathbb{R}^3$ denotes the global body orientation, $\boldsymbol{\theta}_t^{\text{body}} \in \mathbb{R}^{63}$ denotes the local body joint rotations, $\mathbf{r}_t^{\text{neck}} \in \mathbb{R}^3$ denotes the FLAME neck rotation, $\boldsymbol{\theta}_t^{\text{jaw}} \in \mathbb{R}^3$ denotes the jaw rotation, $\boldsymbol{\psi}_t \in \mathbb{R}^{50}$ denotes the facial expression coefficients, and $\boldsymbol{\theta}_t^{\text{rhand}}, \boldsymbol{\theta}_t^{\text{lhand}} \in \mathbb{R}^{45}$ denote the right and left hand joint rotations, respectively. Thus, the augmented frame-wise feature dimension is $D = 212$. Accordingly, the augmented motion sequence for gloss g_k is denoted as

$$\mathbf{X}_{\text{data}}^{(k)} = [\mathbf{x}_1^{(k)}, \dots, \mathbf{x}_{T_k}^{(k)}] \in \mathbb{R}^{T_k \times 212}.$$

D.3 Data Quality Control

We describe in greater detail the data quality control procedure outlined in Section 3.1. Fig. 8 presents representative examples of the five filtering and preprocessing steps, highlighting the rationale behind each criterion and its role in the overall data curation process. First, since each video is intended to correspond to a single lexical item, we discard samples longer than 10 seconds, as such videos often include irrelevant motions or unrelated content. As illustrated in Fig. 8-(a), some videos contain an isolated signing of the target word followed by an explanatory segment. Since these samples do not align with our objective of collecting isolated sign clips, we remove them from the dataset. Second, for datasets with existing signer annotations [80, 39], we re-estimate signer bounding boxes using YOLOv8 [29] to replace the original YOLOv3-based annotations [60] (see Fig. 8). Samples for which reliable signer detection cannot be obtained are discarded. Third, to ensure accurate estimation of facial expressions and hand movements, we retain only front-view frames while excluding side-view segments. (see Fig. 8-(c)). Specifically, using the notation defined in Eq. 1, we discard frames satisfying both $|\mathbf{r}_t^{\text{body}}| > \tau$ and $|\mathbf{r}_t^{\text{neck}}| > \tau$, where $\mathbf{r}_t^{\text{body}}$ and $\mathbf{r}_t^{\text{neck}}$ denote the yaw angles extracted from the root body and neck rotations, respectively, via Euler-angle decomposition; we set $\tau = 0.7$. Next, we remove non-signing segments and frames in which the signer changes within a video. As shown in Fig. 8-(d), some videos contain a trailing explanatory segment for the target word, which we exclude together with any signer-switching portions. We extract identity features using OSNet [96] and compute the cosine similarity with respect to a reference frame. Frames with similarity values below a predefined threshold are treated as scene transitions and discarded. Finally, to enforce structural consistency within each gloss, we split videos into dominant and non-dominant samples. We extract SMPL-X [57] based motion sequences and compute pairwise similarity using subsequence dynamic time warping (DTW) [50] by aligning video prefixes to candidate segments from other samples. Based on KNN average similarity scores, videos with low similarity to their neighbors are classified as non-dominant, while highly similar videos are regarded as dominant.

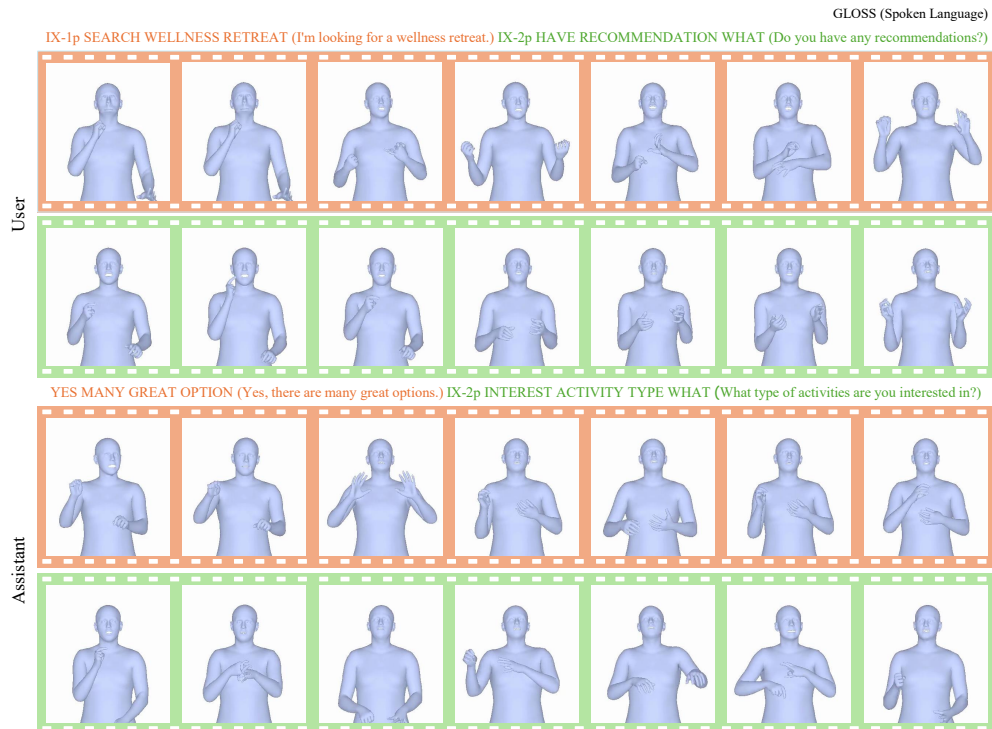


Figure 10: Visualized examples of SIGNAVOX-U. The colors of the generated frames indicate their direct correspondence with the highlighted text.

D.4 Data Visualization

This section provides representative visualizations to qualitatively illustrate the structure and annotation format of the constructed dataset. Fig. 9 shows gloss-level examples of isolated sign clips in SIGNAVOX-W, presenting both the original video frames and their corresponding 3D representations. For visualization, we map the frame-level motion annotations to SMPL-X meshes and render them as 3D representations. These examples show that sign clips collected from diverse sources are aligned under a unified 3D motion representation, while preserving gloss-specific hand trajectories, arm configurations, body postures, and temporal articulation patterns.

Fig. 12 shows a sentence-level annotation example from SIGNAVOX-U. A single conversation turn in SIGNAVOX-U may contain multiple sentences, where each sentence consists of a spoken-language utterance, its corresponding gloss sequence, and the generated 3D sign motion. In the figure, user and assistant turns are shown separately, and the text span of each sentence is linked to the generated sign motion frames using the same color. This illustrates that SIGNAVOX-U is not merely a continuous motion dataset, but provides structured alignment among conversation turns, sentences, glosses, and 3D sign motion.

D.5 SIGNAVOX Annotation

In this section, we describe the annotation structure of the SIGNAVOX, as illustrated in Fig. 11. The primary keys in SIGNAVOX-W include “gloss”, “source info”, “segment”, “enrichment”, “is dominant”, “core span”, “facial expression”, “body”, “rhands” and “lhands”. The “gloss” key specifies the gloss label of each video, enabling retrieval when constructing sentence-level sequences. The “source info” key contains metadata about the original source video. The “segment” key records information about the cropped interval extracted from the source video, together with the signer bounding box. Since datasets such as MS-ASL are built from YouTube videos, the source-level information and the segment-level information may differ; we retain both for clarity and traceability. In addition, following the method proposed in Section ??, we explicitly annotate the span corresponding to the core articulation frames of each sign. Finally, the “enrichment” key provides the linguistic meaning associated with the sign video. Each video-related 3D annotation is flattened into a one-dimensional array. Following the notation introduced in Section 3.1. The “body”, “facial expression”, “rhands”, and “lhands” keys corresponding to θ^{body} , $[\psi, \theta^{\text{jaw}}]$, θ^{rhand} and θ^{lhand} , respectively.



```

{
  'id': 'SignASL_000398',
  'global_id': 56887,
  'gloss': 'ACCEPT',
  'is_clip': False,
  'source_info': {
    'source': 'SignASL',
    'url':
      'https://media.signbsl.com/videos/asl/aslsignbank/mp4/ACCEPT-2045.mp4',
    'width': 656,
    'height': 370,
    'fps': 23.97,
    'duration': 2.04,
    'total_frame_count': 49
  },
  'segment': {
    'start_frame': 0,
    'end_frame': 48,
    'xyxy': [208.45, 49.96, 489.43, 365.66],
    'xywhn': [0.5319, 0.5616, 0.4283, 0.8532],
    'ref': 'source'
  },
  'enrichment': {
    'meaning': [
      'consider or hold as true'
    ],
    'pos': None,
    'synonyms': None
  },
  'is_dominant': True,
  'core span': [24, 37],
  'body': [[2.9185 -0.0191 0.0368, -0.1813, ...], ... ], # Frame num X 66
  'facial expression': [[-0.1404, 2.795, 0.1629, -0.1588, ...], ... ], # Frame num X 53
  'rhands': [[0.0015, -0.6596, 0.8394, 0.3443, ...], ... ], # Frame num X 45
  'lhands': [[0.0263, -0.6939, 0.944, 0.3369, ...], ... ] # Frame num X 45
}

```

Figure 11: The SIGNAVOX-W annotation format. We provide the SIGNAVOX-W dataset in JSON format.

SIGNAVOX-U is organized at the dialogue-turn level. The “conversation” key contains entries structured into “user” and “assistant” turns. For each turn, we provide the spoken language and gloss annotations at the sentence level. In addition, the corresponding 3D sign-language parameters for each gloss sequence are also organized at the sentence level.

D.6 Licensing

Our dataset will first be released under the CC BY-NC-SA (Attribution-NonCommercial-Share-Alike) license for research purposes. Specifically, we will release the SMPL-X/FLAME/MANO annotation and provide the

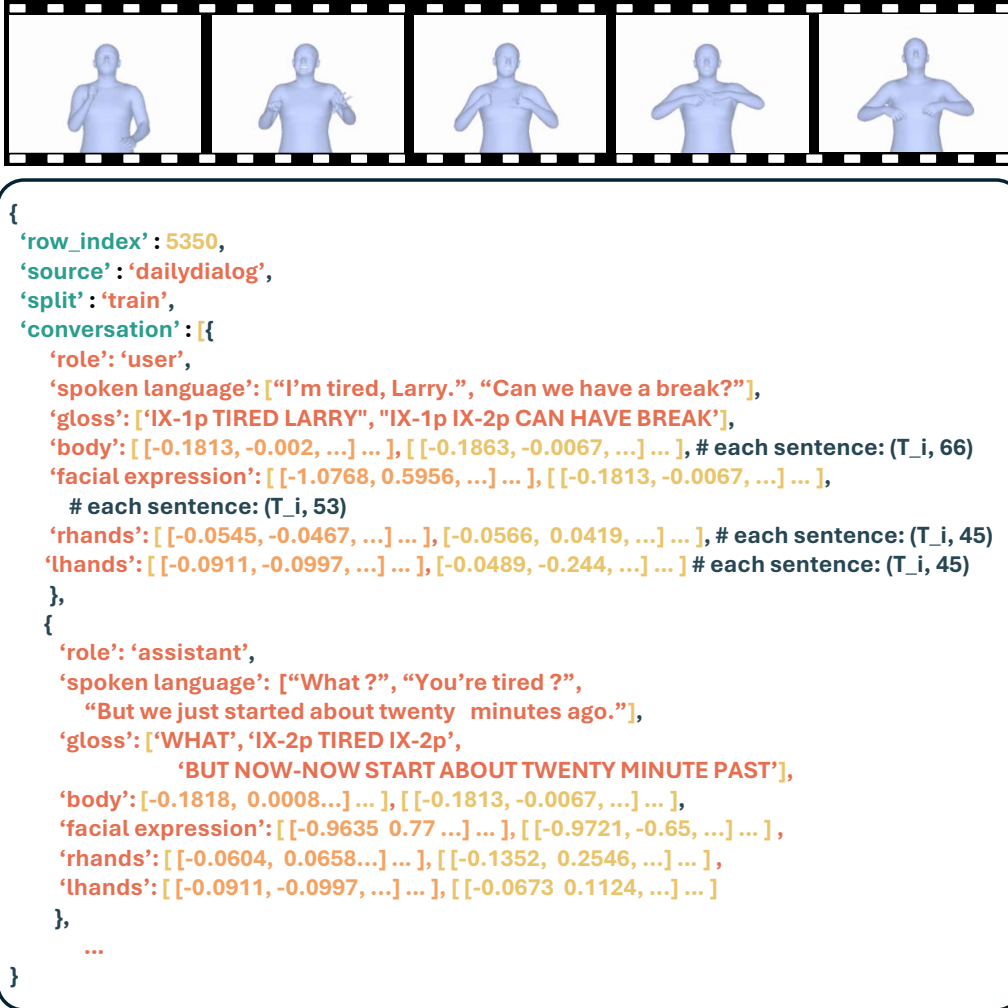


Figure 12: The SIGNAVOX-U annotation format. We provide the SIGNAVOX-U dataset in JSON format. T_i is a number of sentence's frames.

instruction to extract the data instead of distributing the raw videos. We also elaborate on the license of the data source we used in our dataset collection:

- **MS-ASL** [80]. Microsoft Research dataset license terms (dataset-specific; research use).
- **WLASL** [39]. Computational Use of Data Agreement (C-UDA-1.0).
- **SigningSavvy** [67]. Accessed under the website Terms of Service; we do not redistribute original content.
- **Signbank** [27]. Creative Commons Attribution–NonCommercial–NoDerivatives 4.0 International (CC BY-NC-ND 4.0)
- **Spreadthesign** [25]. Administered by the non-profit European Sign Language Centre; accessed under the website Terms of Service, and we do not redistribute original media.
- **SignASL** [70]. An online ASL dictionary with copyright notice (“ASL Sign Dictionary ©2013–2026”); the site aggregates sign videos from multiple sources.
- **ASLLRP** [52]. Provided by Boston University; Terms of Use allow research/educational use only, prohibit commercial use without permission, and restrict redistribution.
- **How2Sign** [11]. Creative Commons Attribution-NonCommercial 4.0 International License.

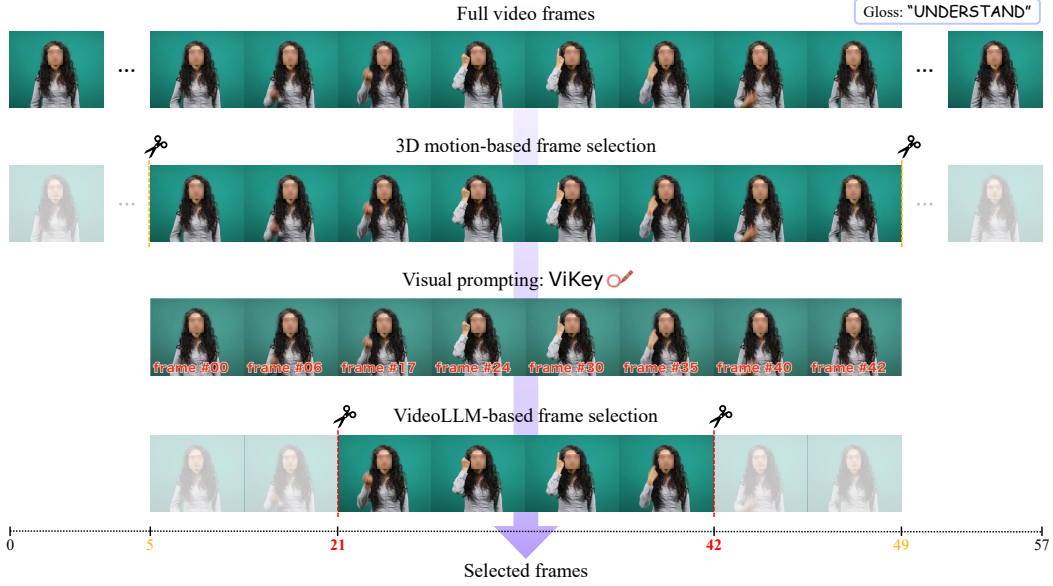


Figure 13: Overview of our frame selection pipeline. A coarse 3D motion-based stage first narrows the candidate range, and a VideoLLM with visual frame-index prompting further refines the start and end boundaries of the core articulation

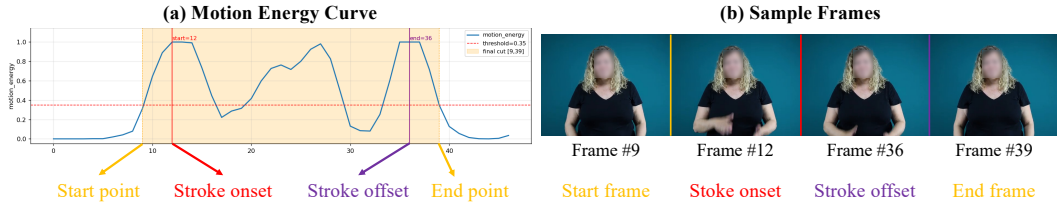


Figure 14: Example of motion-based frame selection. (a) The motion energy curve used to estimate the temporal boundaries of the core articulation. (b) Sample frames corresponding to the estimated start point (t^{start}), stroke onset (t^{on}), stroke offset (t^{off}), and end point (t^{end}). This video represents the sign for “ACADEMICS”

E Details of Frame Selection

In this section, we describe in detail our method for selecting frames corresponding to the core articulation. The overall pipeline, which combines signer motion and a VideoLLM-based approach, is illustrated in Fig. 13. Further details of the prompts used for the VideoLLM are provided in Sec. J.1.

E.1 Energy-Based Preparation and Retraction Trimming

To initially remove preparatory and ending motions from sign clips, we employ a bidirectional trimming method that combines arm/hand-centered motion energy with arm-posture gating. Specifically, we first apply Savitzky–Golay smoothing [66] to the upper-body, arm, and hand features, and then compute motion energy from the first- and second-order temporal differences. Given a smoothed motion feature sequence $\mathbf{X} = \{\mathbf{x}_t\}_{t=1}^T$, we define the raw frame-wise motion-energy score as

$$E_t = \frac{\lambda_v}{D} \|\Delta \mathbf{x}_t\|_2^2 + \frac{\lambda_a}{D} \|\Delta^2 \mathbf{x}_t\|_2^2, \quad (8)$$

where D is the feature dimension, and $\lambda_v = 1.0$ and $\lambda_a = 0.5$ weight the velocity and acceleration terms. For boundary frames where temporal differences are not directly defined, we pad the nearest valid difference values.

We then robustly normalize E_t into $\tilde{E}_t \in [0, 1]$ using quantile-based scaling and compute an arm-posture gate $h_t \in [0, 1]$ from the normalized wrist-to-shoulder height. The final trimming score, $\bar{E}_t = \tilde{E}_t \cdot h_t$, suppresses spurious motion responses from low-arm postures while preserving high-energy signing regions.

We determine the trimming boundaries using a continuity-confirmed threshold criterion. Instead of selecting the first frame that crosses the threshold, we define the onset boundary as the end of the first stable high-energy interval. This choice avoids retaining early arm-raising frames that may exceed the threshold before the signer reaches a sufficiently articulated signing posture. Formally, let \bar{E}_t denote the normalized and gated motion-energy score, θ the threshold, and $n = 3$ the minimum number of consecutive frames required by the continuity condition. The stroke onset t^{on} is defined as

$$t^{\text{on}} = \min \{t + n - 1 \mid t \in \{1, \dots, T - n + 1\}, \forall i \in \{0, \dots, n - 1\}, \bar{E}_{t+i} \geq \theta\}. \quad (9)$$

Thus, t^{on} corresponds to the confirmed onset boundary after the motion energy has remained above the threshold for n consecutive frames.

Similarly, the stroke offset t^{off} is estimated by applying the same continuity-confirmed criterion in the reverse temporal direction. Equivalently, in the original temporal order, it is defined as the beginning of the last stable high-energy interval:

$$t^{\text{off}} = \max \{t - n + 1 \mid t \in \{n, \dots, T\}, \forall i \in \{0, \dots, n - 1\}, \bar{E}_{t-i} \geq \theta\}. \quad (10)$$

Finally, to avoid overly aggressive trimming, we add a temporal margin m before and after the estimated onset and offset boundaries. We set $m = 3$ in all experiments. The start and end points of the retained interval are defined as

$$t^{\text{start}} = \max(1, t^{\text{on}} - m), \quad t^{\text{end}} = \min(T, t^{\text{off}} + m), \quad (11)$$

where T denotes the total number of frames. Fig. 14 illustrates these boundary definitions on the motion-energy curve.

E.2 Posture Cue and Hyperparameters

For posture-based trimming, we compute a wrist-height cue from the SMPL-X joint sequence. Let $a \in \{L, R\}$ denote the left or right side, and let $\mathbf{j}_t^{\text{pelvis}}$, $\mathbf{j}_t^{\text{neck}}$, $\mathbf{j}_t^{\text{shoulder},a}$, and $\mathbf{j}_t^{\text{wrist},a}$ denote the pelvis, neck, shoulder, and wrist joints at frame t , respectively. Here, the y -axis denotes the vertical direction. We first define the torso height as

$$H_t = \max \left(\left| j_{t,y}^{\text{neck}} - j_{t,y}^{\text{pelvis}} \right|, 10^{-6} \right), \quad (12)$$

and normalize the wrist-to-shoulder height by this value:

$$r_t^a = \frac{j_{t,y}^{\text{wrist},a} - j_{t,y}^{\text{shoulder},a}}{H_t}. \quad (13)$$

We then use $r_t^{\text{max}} = \max(r_t^L, r_t^R)$ as a scale-normalized estimate of whether at least one hand is raised into an active signing posture. For boundary detection, we form a direction-specific posture gate $g_t^d = \mathbb{1}[r_t^{\text{max}} \geq \tau_{\text{post}}^d]$, where $d \in \{\text{on}, \text{off}\}$ denotes the onset and offset scans. This gate is applied to the normalized motion energy to suppress spurious responses from arm-down postures.

The trimming procedure uses a small set of fixed hyperparameters. We set the activity threshold to $\theta_{\text{act}} = 0.35$ and use a low-motion cutoff $\theta_{\text{low}} = 0.4$ for auxiliary boundary protection. The posture thresholds are set to $\tau_{\text{post}}^{\text{on}} = 0.6$ for the onset scan and $\tau_{\text{post}}^{\text{off}} = 0.25$ for the offset scan, reflecting the different posture patterns of preparation and retraction motions. To avoid overly short or unstable clips, we require the retained segment to contain at least $T_{\text{min}} = 8$ frames and remove boundary regions only when they are longer than $B_{\text{min}} = 5$ frames. We use a temporal margin of $m = 3$ frames on both sides of the estimated onset and offset. For smoothing and energy computation, we use a Savitzky–Golay filter with window size $w_{\text{SG}} = 7$ and polynomial order $p_{\text{SG}} = 2$, and set the velocity and acceleration weights to $\lambda_v = 1.0$ and $\lambda_a = 0.5$, respectively. Middle inactive-region removal is disabled, and the continuity criterion is fixed to $n = 3$ consecutive frames for both onset and offset detection.

For the subsequent Video-LLM refinement stage, we use the pretrained Qwen3-VL model [3] without additional fine-tuning. Given the coarsely trimmed clip, the model is asked to identify the contiguous frame interval corresponding to the core lexical articulation. To make frame-level selection explicit, we overlay frame indices on the input video frames. All queries are performed with greedy decoding by setting the temperature to 0.0; top- p is kept at 0.95 in the decoding configuration.

F Details of Isolated to Continuous

F.1 Details of Data Setup.

This section details the gloss normalization and filtering rules used to construct the training pairs described in Sec. 3.2. We use ASLLRP [52] as continuous signing supervision and organize its annotations into sentence-level

Table 9: Gloss conventions adopted for dataset construction.

Category	Gloss	Example	Explanation
English-based glosses	-	THANK-YOU	Used to separate words if the English translation of a single sign requires more than one.
Fingerspelling	fs-	fs-J-O-H-N	Fingerspelled word.
	#	#-E-A-R-L-Y	Fingerspelled loan sign. Represented with fingerspelling.
Name Signs	ns-	ns-P-A-R-I-S	Used for proper nouns (<i>e.g.</i> people, places, etc.)
Pronoun	IX-[person]	IX-1p	First-person pronoun (I / WE).
		IX-2p	Second-person pronoun referring to the addressee (YOU).
		IX-3p	Third-person pronoun (HE / SHE / THEY).
Possessive	POSS-[person]	POSS-1p	First-person possessive marker (MY / OUR).
		POSS-2p	Second-person possessive marker (YOUR).
		POSS-3p	Third-person possessive marker (HIS / HER / THEIR).
Emphatic reflexive	SELF-[person]	SELF-1p	First-person emphatic reflexive marker (MYSELF / OURSELVES).
		SELF-2p	Second-person emphatic reflexive marker referring to the addressee (YOURSELF / YOURSELVES).
		SELF-3p	Third-person emphatic reflexive marker (HIMSELF / HERSELF / THEMSELVES).

utterances. Following the SignStream conventions used in ASLLRP, we normalize gloss labels and summarize the filtering rules in Table 9. To improve consistency with SIGNAVOX-W retrieval and downstream gloss-pair training, we normalize the ASLLRP gloss sequences before retrieving corresponding isolated clips.

We remove translation-like or annotative tokens, such as quoted forms and bracketed tags (*e.g.*, 5"wow", [false-start]). In contrast, we retain grammatical markers that are important for sign language structure (*e.g.*, IX-*, POSS-*, fs-*, #*, ns-*, and ns-fs-*). We further remove classifier-related tokens (*e.g.*, DCL, TCL, PCL, SCL, BCL, and their variants), since they exhibit high variability and limited consistency across annotations. To improve annotation consistency, we also simplify deictic, possessive, and locus-indexed forms by removing locus suffixes where possible (*e.g.*, IX-3p:i → IX-3p, IX-1oc:j → IX-1oc, and POSS-3p:i → POSS-3p). Finally, we remove discourse-management or meta-level markers (*e.g.*, NEXT-TOPIC, CURRENT-TOPIC).

After normalization, we filter noisy English-gloss pairs using several criteria. We discard samples whose gloss sequence becomes empty after preprocessing, as well as cases where the gloss sequence is disproportionately short relative to the English sentence (*e.g.*, more than 20 English words but at most 3 gloss tokens). We further exclude samples with very low character n-gram TF-IDF similarity between English and gloss, which often indicates weak surface correspondence. To complement these heuristic filters, we also use GPT-4o [53] to assess semantic alignment and discard pairs judged to have substantially mismatched meanings.

F.2 Consistency Analysis

During *BRAID* training, we construct 14 different pseudo inputs for the same gloss pair and train the model to recover a natural co-articulatory transition between the two glosses. Although these pseudo inputs vary across seeds, the underlying transition required by the same gloss pair should remain similar. Therefore, if the refined outputs generated from different pseudo inputs exhibit consistent motion patterns, it suggests that the model captures the transition structure associated with the gloss pair rather than overfitting to seed-specific input noise.

To quantify this behavior, we measure the cosine similarity between refined motions generated from different pseudo-input seeds. For each gloss pair or sentence, we compute all pairwise cosine similarities among the 14 seed outputs and summarize them by their mean similarity. Fig. 15 shows the distribution of these per-instance consistency scores for both gloss-pair-level and sentence-level predictions. The gloss-pair predictions show high consistency across pseudo seeds, with a mean similarity of 0.715. This indicates that, despite receiving different pseudo inputs, *BRAID* produces mutually similar refined transitions for the same gloss pair. Sentence-level predictions also exhibit a consistent trend, with a mean similarity of 0.579, although the score is lower due to the longer temporal span and greater motion variability at the sentence level. Overall, these results support that *BRAID* learns stable co-articulatory motion patterns conditioned on the underlying gloss pair or sentence, rather than producing outputs that vary arbitrarily with the pseudo-input seed.

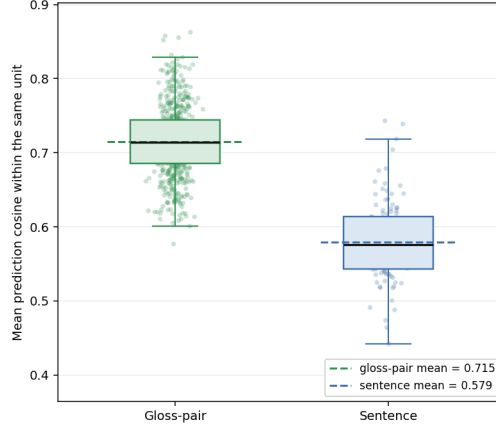


Figure 15: Consistency of *BRAID* predictions across varying pseudo-input seeds. The box-plots illustrate the distribution of mean pairwise cosine similarities for motions generated from different random seeds, evaluated at both the gloss-pair and sentence levels.

F.3 Duration Predictor

We provide additional details for the two duration predictors, $\mathcal{D}_{\text{gloss}}$ and $\mathcal{D}_{\text{sent}}$, used in Sec. 3.2. Both predictors estimate a global temporal scale \hat{s} and a gloss-wise duration allocation $\hat{\mathbf{w}}$, from which integer target lengths are derived for resampling and downstream diffusion refinement.

Predictor architectures. The gloss-pair predictor $\mathcal{D}_{\text{gloss}}$ is implemented as a 4-layer MLP with hidden dimension 256. Its input consists of segment-level motion summaries from the two isolated gloss clips, local boundary features around the gloss transition, a boundary-jump feature, and simple length statistics. The model predicts the global scale \hat{s} and a two-way split $\hat{\mathbf{w}} \in \mathbb{R}^2$ for the pair.

The sentence-level predictor $\mathcal{D}_{\text{sent}}$ uses a token-based Transformer encoder, where each gloss segment is represented as one token. Each token encodes segment-level motion statistics and length-related features, and valid gloss tokens are processed with padding masks. The encoded tokens are used to predict both the sentence-level scale \hat{s} and the gloss-wise allocation $\hat{\mathbf{w}} \in \mathbb{R}^K$ over the valid K glosses. We set the maximum number of glosses to $K_{\text{max}} = 32$, which covers almost all utterances in our training data.

For both predictors, the scale prediction is bounded by clamping $\hat{s} \in [-3, 3]$, which limits the multiplicative length rescaling $\exp(\hat{s})$. We also initialize the output heads to produce near-identity rescaling and approximately uniform duration allocation at the beginning of training.

Training targets. For both predictors, the target scale is defined as

$$s = \log(T_{\text{tgt}}/T_{\text{src}}),$$

where T_{src} and T_{tgt} denote the input and target motion lengths. For gloss pairs, the target split is directly obtained from the target boundary position. For sentence-level prediction, we derive per-gloss target lengths by assigning inter-gloss gaps to neighboring glosses using midpoint boundaries, which yields a length allocation \mathbf{w}^{GT} whose entries sum to one.

Both predictors are trained with a scale loss and a split-allocation loss:

$$\mathcal{L}_{\text{dur}} = \rho_{\tau}(s - \hat{s}) + \lambda_{\text{split}} \text{CE}(\hat{\mathbf{w}}, \mathbf{w}^{\text{GT}}),$$

where ρ_{τ} is the pinball quantile loss [33]. We use a slightly larger quantile for the sentence-level predictor to reduce under-prediction, since sentence-level length errors propagate to all downstream stitched segments.

Inference-time duration plan. At inference time, the predicted scale determines the total output length, while the predicted allocation determines the per-gloss lengths. For a gloss pair, $\mathcal{D}_{\text{gloss}}$ directly predicts the total pair length and the boundary position between the two glosses. For a full sentence, $\mathcal{D}_{\text{sent}}$ first predicts the total sentence length and then distributes it across the K glosses according to $\hat{\mathbf{w}}$. The resulting real-valued allocations are rounded with a sum-preserving correction and constrained by a minimum length per gloss. The final integer plan $\{\hat{T}_k\}_{k=1}^K$ is used consistently for pairwise diffusion refinement and cosine-window stitching, ensuring that the stitched sentence length matches the predicted sentence-level plan.

Table 10: Duration predictor hyperparameters.

	$\mathcal{D}_{\text{gloss}}$	$\mathcal{D}_{\text{sent}}$
Architecture	4-layer MLP	3-layer Transformer
Hidden / model dim	256	256
FFN dim	–	512
Attention heads	–	4
Boundary window	5 frames	5 frames
Max glosses K_{max}	2	32
Motion dim D	206	206
Optimizer	AdamW	AdamW
Learning rate	10^{-3}	10^{-3}
Weight decay	10^{-4}	10^{-4}
Batch size	64	64
Epochs	50	60
LR schedule	cosine	cosine
Grad. clipping	1.0	1.0
Quantile τ	0.55	0.60
λ_{split}	1.0	1.0
Scale clamp	$[-3, 3]$	$[-3, 3]$

Hyperparameters. Table 10 summarizes the main hyperparameters used for both duration predictors.

F.4 Details of BRAID

Hyperparameters We trained our model using H100 GPUs, and the detailed hyperparameters are provided in Table 11.

We expand on the components introduced in the main text: the boundary-inpainting forward process, the masked part-weighted objective $\mathcal{L}_{\text{braid}}$, and the inference-time composition. All notation matches the main paper.

Part-Wise Feature Weight Vector ω_{part} Sign language is dominated by hand articulation and modulated by facial expression, so we assign a non-uniform per-feature weight $\omega_{\text{part}} \in \mathbb{R}_{>0}^D$ that emphasizes hand and face dimensions. Let $D = D_{\text{body}} + D_{\text{face}} + D_{\text{hand}}$ partition the feature axis into body, face (expression + jaw), and hand (left + right) sub-blocks. We define

$$\omega_{\text{part}}[d] = \begin{cases} \omega_{\text{body}} & \text{if } d \in \mathcal{I}_{\text{body}}, \\ \omega_{\text{face}} & \text{if } d \in \mathcal{I}_{\text{face}}, \\ \omega_{\text{hand}} & \text{if } d \in \mathcal{I}_{\text{hand}}, \end{cases} \quad (14)$$

with $(\omega_{\text{body}}, \omega_{\text{face}}, \omega_{\text{hand}}) = (1.0, 3.0, 15.0)$ in our experiments

Masked Reconstruction Loss $\mathcal{L}_{\text{recon}}$ $\mathcal{L}_{\text{recon}}$ is a Smooth-L1 loss applied only on the supervised inpainting region $\{i : M_i = 1\}$, with per-feature weighting by ω_{part} :

$$\mathcal{L}_{\text{recon}}(\hat{\mathbf{X}}_0, \mathbf{X}_0; \mathbf{M}, \omega_{\text{part}}) = \frac{\sum_{i=1}^{\tilde{T}} \sum_{d=1}^D M_i \omega_{\text{part}}[d] \rho_{\beta}(\hat{X}_{0,i,d} - X_{0,i,d})}{\sum_{i=1}^{\tilde{T}} \sum_{d=1}^D M_i \omega_{\text{part}}[d]}, \quad (15)$$

where $\rho_{\beta}(\cdot)$ is the elementwise Smooth-L1 (Huber) function with transition β :

$$\rho_{\beta}(u) = \begin{cases} \frac{1}{2\beta} u^2, & |u| < \beta, \\ |u| - \frac{\beta}{2}, & |u| \geq \beta. \end{cases} \quad (16)$$

We use $\beta = 1.0$.

Masked Velocity Regularization \mathcal{L}_{vel} The velocity regularization is computed on first-order temporal differences. Let $\Delta \mathbf{X}_{0,i} = \mathbf{X}_{0,i+1} - \mathbf{X}_{0,i}$ (and similarly $\Delta \hat{\mathbf{X}}_{0,i}$) for $i = 1, \dots, \tilde{T} - 1$. The velocity-domain mask retains only differences between two supervised frames:

$$M_i^{\Delta} = M_i \cdot M_{i+1}, \quad i = 1, \dots, \tilde{T} - 1. \quad (17)$$

Then

$$\mathcal{L}_{\text{vel}}(\Delta \hat{\mathbf{X}}_0, \Delta \mathbf{X}_0; \mathbf{M}^{\Delta}, \omega_{\text{part}}) = \frac{\sum_{i=1}^{\tilde{T}-1} \sum_{d=1}^D M_i^{\Delta} \omega_{\text{part}}[d] \rho_{\beta}(\Delta \hat{X}_{0,i,d} - \Delta X_{0,i,d})}{\sum_{i=1}^{\tilde{T}-1} \sum_{d=1}^D M_i^{\Delta} \omega_{\text{part}}[d]}. \quad (18)$$

This penalizes per-frame jerk specifically on the boundary region, where co-articulatory transitions matter most.

Table 11: Training hyperparameters of the gloss-level diffusion model.

Hyperparameter	Value
<i>Architecture</i>	
Latent / model dimension	512
Transformer layers	6
Attention heads	8
Feed-forward size	2048
Dropout	0.1
Positional encoding	RoPE
Hand head depth	4
Hand cross-attention layers / heads	2 / 4
<i>Diffusion</i>	
Diffusion steps T	1000
Loss weighting	Min-SNR- γ
Min-SNR γ	5.0
EMA decay	0.9999
Inpaint radius (min / max)	10 / 30
Inference inpaint radius	10
<i>Optimization</i>	
Optimizer	AdamW
Learning rate	1×10^{-4}
Weight decay	1×10^{-4}
Global batch size	256
Epochs	100
Gradient clipping (max-norm)	1.0
<i>Loss weights</i>	
Latent reconstruction λ_{latent} (L2)	1.0
Parameter reconstruction λ_{param} (smooth-L1)	1.0
Velocity λ_{vel}	0.5
Body part weight	1.0
Face part weight	3.0
Hand part weight	15.0

Min-SNR- γ Timestep Weighting $w(t)$ We adopt the Min-SNR- γ scheme of Hang *et al.* [24] to prevent low-SNR diffusion steps from dominating the gradient. With signal-to-noise ratio $\text{SNR}(t) = \bar{\alpha}_t / (1 - \bar{\alpha}_t)$,

$$w(t) = \frac{\min(\text{SNR}(t), \gamma)}{\text{SNR}(t)}. \quad (19)$$

We set $\gamma = 5$, sample $t \sim \mathcal{U}\{1, \dots, T\}$ with $T = 1000$, and apply $w(t)$ as a per-sample multiplier on $\mathcal{L}_{\text{recon}}$ and \mathcal{L}_{vel} , recovering the full objective in the main text.

F.5 Inference-Time Composition

At inference we use DDIM sampling [71] with $\eta = 0$ on a respaced subset of $S \ll T$ timesteps. The reverse process is initialized only inside the boundary region:

$$\mathbf{X}_{t_S} = \mathbf{M} \odot \boldsymbol{\eta} + (1 - \mathbf{M}) \odot \tilde{\mathbf{X}}^{(k, k+1)}, \quad \boldsymbol{\eta} \sim \mathcal{N}(\mathbf{0}, \mathbf{I}). \quad (20)$$

At each respaced step $t_s \rightarrow t_{s-1}$, given $\hat{\mathbf{X}}_0 = G_\theta(\mathbf{X}_{t_s}, t_s, \mathbf{c}, \mathbf{M})$, the prediction is first composed with the temporal context to keep $M_i = 0$ frames pinned to the duration-adjusted pseudo sequence,

$$\hat{\mathbf{X}}_0 \leftarrow \mathbf{M} \odot \hat{\mathbf{X}}_0 + (1 - \mathbf{M}) \odot \tilde{\mathbf{X}}^{(k, k+1)}, \quad (21)$$

and the deterministic DDIM update is then applied with $\boldsymbol{\epsilon}_\theta = (\mathbf{X}_{t_s} - \sqrt{\bar{\alpha}_{t_s}} \hat{\mathbf{X}}_0) / \sqrt{1 - \bar{\alpha}_{t_s}}$,

$$\mathbf{X}_{t_{s-1}} = \sqrt{\bar{\alpha}_{t_{s-1}}} \hat{\mathbf{X}}_0 + \sqrt{1 - \bar{\alpha}_{t_{s-1}}} \boldsymbol{\epsilon}_\theta. \quad (22)$$

The final refined gloss-pair motion is the converged sample $\hat{\mathbf{X}}_0^{\text{comp}}$, which is used as the building block for sentence-level stitching across all consecutive gloss pairs.

G Details of Spoken Language to Gloss

G.1 Hyperparameters

Anonymization is applied only to the retrieval index and retrieval queries; the original English utterances, retrieved demonstrations, and target gloss sequences are kept unchanged in the LLM prompt. Named entities are detected using spaCy [28] and replaced with coarse placeholders: PERSON \rightarrow “someone,” ORG \rightarrow “some organization,” GPE/LOC \rightarrow “some place,” FAC \rightarrow “some facility,” and NORP \rightarrow “some group.” For overlapping entity spans, we retain the longest span, and apply the same rule when multiple spans share the same start position.

For first-stage retrieval, BM25 uses $k_1 = 1.5$ and $b = 0.75$. SPLADE representations are computed with a maximum input length of 256 tokens, retaining up to 128 document terms and 64 query terms. BM25 and SPLADE scores are normalized independently with per-query min-max normalization and combined as

$$s_{\text{first}} = \alpha s_{\text{BM25}} + (1 - \alpha) s_{\text{SPLADE}},$$

where $\alpha = 0.35$. We pass the top 30 first-stage candidates to the second-stage reranker, and compute the final score as

$$s_{\text{final}} = 0.85 \cdot s_{\text{reranker}} + 0.15 \cdot s_{\text{first}}.$$

Finally, we deduplicate candidates using normalized English sentences and select the top 6 examples for the translation-memory prompt.

G.2 Experimental Details

To evaluate the performance of the gloss translator, we construct a retrieval set of 100 examples and conduct experiments on the remaining 1,261 spoken language-gloss pairs. For a more appropriate quantitative assessment of semantic fidelity and grammatical correctness, finger-spelled expressions are normalized into a single lexical token prior to evaluation (*e.g.* ns-fs-PARIS \rightarrow PARIS). Since the official implementation of the previous work [91] is not publicly available, we reproduced its methodology based on the descriptions provided in the work. We will publicly release both the evaluation set and the retrieval set.

H Details of Sign Language Conversational Model

H.1 Retrieval-Based Semantic Evaluation

We propose a hybrid retrieval-based evaluation protocol to assess the semantic recoverability of generated sign motions. Instead of directly decoding the generated motion with a learned sign-to-text model, we compare the input motion against two complementary memory banks: the sentence-level SIGNAVOX-U memory and the gloss-level SIGNAVOX-W memory.

Given an input sentence-level motion sequence x , we first extract a motion feature embedding using an encoder $\phi(\cdot)$. We then retrieve sentence-level candidates from the SIGNAVOX-U memory by computing cosine similarity between the input motion and each sentence motion u_i :

$$s_U(x, u_i) = \phi(x)^\top \phi(u_i), \tag{23}$$

where u_i denotes a sentence-level motion sequence in SIGNAVOX-U. Since each SIGNAVOX-U sentence is paired with spoken-language text and gloss annotations, the retrieved candidates provide pseudo translation candidates for the input motion.

In parallel, we perform gloss-level retrieval using SIGNAVOX-W. For each retrieved sentence candidate, we divide the input motion x into K temporal segments according to the length of the candidate gloss sequence. Each segment is then compared with the SIGNAVOX-W gloss prototype memory, producing gloss-level evidence $\hat{g}_W(x)$ that indicates which gloss sequence the input motion locally resembles.

For each SIGNAVOX-U candidate u_i , we compute a final hybrid score by combining sentence-level motion similarity, gloss-level consistency, and gloss retrieval confidence:

$$S(x, u_i) = \lambda_U \tilde{s}_U(x, u_i) + \lambda_G \text{F1}(\hat{g}_W(x), g_i) + \lambda_C c_W(x), \tag{24}$$

where $\tilde{s}_U(x, u_i)$ is the min-max normalized sentence-level retrieval score among the top- k candidates, g_i is the reference gloss sequence of candidate u_i , $\text{F1}(\hat{g}_W(x), g_i)$ measures token-level overlap between the gloss evidence retrieved from SIGNAVOX-W and the candidate gloss sequence, and $c_W(x)$ denotes the gloss retrieval confidence. We use $\lambda_U = 0.55$, $\lambda_G = 0.40$, and $\lambda_C = 0.05$ by default.

The candidate with the highest hybrid score is selected as the hybrid pseudo translation for the input motion.

Table 12: Upper-bound calibration of the hybrid retrieval-based semantic evaluator on ground-truth assistant test motions.

Setting	MRR	R@1	R@5	R@10	Gloss F1	Gloss BLEU-4	Gloss chrF
GT motion query	0.495	0.415	0.584	0.644	0.479	0.305	0.498

H.2 Implementation Details

Model Configuration. Table 13 summarizes the architecture hyperparameters used for SIGNAVOX. The model uses block-wise autoregressive generation with a Qwen-style causal Transformer decoder and anatomy-factorized flow heads.

Table 13: Architecture hyperparameters of SIGNAVOX.

Component	Value
Motion block size K	8
Body / face / hand embedding chunks	256 / 256 / 256
Transformer hidden size	768
Transformer layers	14
Attention heads	12
Key-value heads	4
FFN intermediate size	2048
Maximum sequence length	2048
Body flow head hidden size	256
Face flow head hidden size	256
Hand flow head hidden size	320
Body / face flow head depth	3
Hand flow head depth	4
Flow head attention heads	4
Sampling steps per block	8
Maximum speakers	8
Maximum turns	32

Training Setup. We train SIGNAVOX in the single-turn response generation setting. Each training example consists of one source sign turn as context and the corresponding target response. The model is trained to generate assistant responses, and context dropout is disabled in this setting. Table 14 summarizes the optimization and data settings.

Table 14: Training hyperparameters for SIGNAVOX.

Hyperparameter	Value
Target role	assistant
Maximum context turns	1
Maximum context slots	1536
Maximum target slots	384
Context dropout probability	0.0
Batch size per GPU	16
Number of GPUs	2
Gradient accumulation	1
Effective batch size	32
Optimizer	AdamW
Learning rate	3×10^{-4}
Adam betas	(0.9, 0.95)
Weight decay	0.01
LR warmup steps	2000
LR schedule	cosine decay
Gradient clipping	1.0
Precision	bfloat16 mixed precision
Maximum training steps	200k
Maximum epochs	120
Selected checkpoint	epoch 119

Loss Weights and Curriculum. Table 15 reports the weights used for the auxiliary losses and curriculum schedules. The model is trained with conditional flow matching as the main motion generation objective, together with boundary prediction, CTC-based gloss planning, post-motion CTC, and landmark gloss supervision.

Table 15: Loss weights and curriculum schedules for SIGNAVOX.

Term	Value
Boundary loss weight λ_{bdry}	0.3
Sentence boundary positive weight	20.0
Turn boundary positive weight	12.0
Boundary-rate calibration weight	0.05
Plan CTC weight λ_{plan}	0.35
Post-motion CTC weight λ_{post}	0.05
Landmark gloss weight λ_{lm}	0.02
Plan-to-flow final weight	0.4
Plan-to-flow warmup	2000–10000 steps
Plan CTC warmup	500–5000 steps
Post CTC / landmark warmup	3000–8000 steps
Hand flow loss weight	1.0

The boundary-rate calibration term aligns the average predicted boundary frequency with the empirical target frequency within each batch:

$$\mathcal{L}_{\text{rate}} = (\bar{p}_{\text{sent}} - \bar{y}_{\text{sent}})^2 + (\bar{p}_{\text{turn}} - \bar{y}_{\text{turn}})^2, \quad (25)$$

where \bar{p}_{sent} and \bar{p}_{turn} denote the mean predicted sentence-end and turn-end probabilities over valid blocks, and \bar{y}_{sent} and \bar{y}_{turn} denote the corresponding target rates.

For plan-to-flow conditioning, the pre-motion gloss planner outputs log probabilities over the gloss vocabulary. We convert them into a soft gloss embedding by taking the expectation over a learned gloss embedding table. The resulting embedding is passed through a projection MLP and added to the flow-head memory. During training, the contribution of this semantic conditioning path is multiplied by a curriculum weight that linearly increases to its final value.

H.3 Loss Definitions

We provide the explicit definitions of the loss terms used to train SIGNAVOX. For a target response Y_ℓ , let B_ℓ denote the ℓ -th K -frame ground-truth motion block, and let C_ℓ be the decoder conditioning memory for that block. Each block is decomposed into anatomical components:

$$B_\ell = [B_\ell^{\text{body}}, B_\ell^{\text{face}}, B_\ell^{\text{hand}}]. \quad (26)$$

Flow matching loss. For each anatomical component $a \in \{\text{body}, \text{face}, \text{hand}\}$, we sample Gaussian noise $x_0^a \sim \mathcal{N}(0, I)$, take the target block component $x_1^a = B_\ell^a$, and sample $\tau \sim \mathcal{U}(0, 1)$. The interpolation point is

$$x_\tau^a = (1 - \tau)x_0^a + \tau x_1^a. \quad (27)$$

The component-wise flow matching loss is

$$\mathcal{L}_{\text{FM}}^a = \mathbb{E}_{\ell, x_0^a, \tau} [\|v_\theta^a(x_\tau^a, \tau; C_\ell) - (x_1^a - x_0^a)\|_2^2]. \quad (28)$$

The total motion generation loss is

$$\mathcal{L}_{\text{FM}} = \mathcal{L}_{\text{FM}}^{\text{body}} + \mathcal{L}_{\text{FM}}^{\text{face}} + \lambda_{\text{hand}} \mathcal{L}_{\text{FM}}^{\text{hand}}. \quad (29)$$

Boundary loss. For each valid block ℓ , the boundary head predicts sentence-end and turn-end probabilities:

$$p_\ell^{\text{sent}} = \sigma(z_\ell^{\text{sent}}), \quad p_\ell^{\text{turn}} = \sigma(z_\ell^{\text{turn}}), \quad (30)$$

with binary targets $y_\ell^{\text{sent}}, y_\ell^{\text{turn}} \in \{0, 1\}$. No-boundary corresponds to $y_\ell^{\text{sent}} = 0$ and $y_\ell^{\text{turn}} = 0$.

Let \mathcal{V} be the set of valid, non-padding blocks. We use weighted binary cross entropy for sentence-end and turn-end prediction:

$$\mathcal{L}_{\text{BCE}}^{\text{sent}} = -\frac{1}{|\mathcal{V}|} \sum_{\ell \in \mathcal{V}} [\alpha_{\text{sent}} y_\ell^{\text{sent}} \log p_\ell^{\text{sent}} + (1 - y_\ell^{\text{sent}}) \log(1 - p_\ell^{\text{sent}})], \quad (31)$$

$$\mathcal{L}_{\text{BCE}}^{\text{turn}} = -\frac{1}{|\mathcal{V}|} \sum_{\ell \in \mathcal{V}} [\alpha_{\text{turn}} y_{\ell}^{\text{turn}} \log p_{\ell}^{\text{turn}} + (1 - y_{\ell}^{\text{turn}}) \log(1 - p_{\ell}^{\text{turn}})]. \quad (32)$$

Here, α_{sent} and α_{turn} are positive-class weights.

To calibrate the predicted boundary frequency, we add a boundary-rate loss:

$$\mathcal{L}_{\text{rate}} = (\bar{p}^{\text{sent}} - \bar{y}^{\text{sent}})^2 + (\bar{p}^{\text{turn}} - \bar{y}^{\text{turn}})^2, \quad (33)$$

where

$$\bar{p}^{\text{sent}} = \frac{1}{|\mathcal{V}|} \sum_{\ell \in \mathcal{V}} p_{\ell}^{\text{sent}}, \quad \bar{y}^{\text{sent}} = \frac{1}{|\mathcal{V}|} \sum_{\ell \in \mathcal{V}} y_{\ell}^{\text{sent}}, \quad (34)$$

and $\bar{p}^{\text{turn}}, \bar{y}^{\text{turn}}$ are defined analogously. The full boundary loss is

$$\mathcal{L}_{\text{bdry}} = \mathcal{L}_{\text{BCE}}^{\text{sent}} + \mathcal{L}_{\text{BCE}}^{\text{turn}} + \lambda_{\text{rate}} \mathcal{L}_{\text{rate}}. \quad (35)$$

Pre-motion CTC planning loss. Let $G = (g_1, \dots, g_J)$ be the target gloss sequence. The pre-motion planning head predicts a block-level gloss posterior sequence P_{plan} before observing the corresponding target motion blocks. Using CTC, the planning loss marginalizes over all monotonic alignments π that collapse to G :

$$\mathcal{L}_{\text{plan}} = -\log \sum_{\pi \in \mathcal{A}(G)} \prod_{\ell=1}^L P_{\text{plan}}(\pi_{\ell} | C_{\ell}), \quad (36)$$

where $\mathcal{A}(G)$ is the set of CTC alignments whose collapse equals G .

Post-motion CTC loss. We also apply a weaker CTC loss to the hidden states after teacher-forced target motion is observed. Let H_{ℓ}^{post} denote the post-motion hidden representation for block ℓ , and let P_{post} be the corresponding gloss posterior sequence. The post-motion CTC loss is

$$\mathcal{L}_{\text{post}} = -\log \sum_{\pi \in \mathcal{A}(G)} \prod_{\ell=1}^L P_{\text{post}}(\pi_{\ell} | H_{\ell}^{\text{post}}). \quad (37)$$

Landmark gloss loss. For a subset of gloss labels, we use approximate landmark block indices indicating where a gloss is centered in the response. Let \mathcal{Q} be the set of valid landmark annotations, where each item (j, q_j) contains the gloss index j and its landmark block index q_j . The landmark loss is

$$\mathcal{L}_{\text{lm}} = -\frac{1}{|\mathcal{Q}|} \sum_{(j, q_j) \in \mathcal{Q}} \log P_{\text{post}}(g_j | H_{q_j}^{\text{post}}). \quad (38)$$

If no valid landmark annotation is available, this term is masked out.

I Additional Experiments Results

I.1 Frame Selection

We evaluate how effectively the proposed frame selection pipeline identifies core articulation frames. To this end, we compare the selected isolated sign segments with gloss-level ground-truth segments from ASLLRP using DTW-MPJPE and DTW-MPVPE. We also report FGD to measure the distributional similarity of motion features, and Length Ratio to quantify the temporal mismatch between the selected segment and the target gloss-level segment. The results are shown in Table 16.

Table 16: Evaluation of articulation-frame selection against ASLLRP gloss-level ground truth.

	DTW MPJPE ↓	DTW MPVPE ↓	FGD ↓	Length Ratio
Raw	0.1070	0.0710	22.12	18.10
Motion-only	0.1005	0.0675	19.89	12.71
VideoLLM-only	0.0931	0.0635	17.03	7.13
Ours	0.0921	0.0629	16.29	5.76

The raw isolated clips show large errors and a severe length mismatch, indicating that they contain substantial redundant frames such as preparation, retraction, and non-signing intervals. Applying motion-based selection reduces both motion error and temporal mismatch, while VideoLLM-only selection further improves all metrics. Our full pipeline achieves the best results across DTW-MPJPE, DTW-MPVPE, and FGD, and substantially reduces the Length Ratio compared with the raw input. These results suggest that coarse motion-based localization and VideoLLM-based refinement are complementary, enabling more accurate selection of core articulation frames.

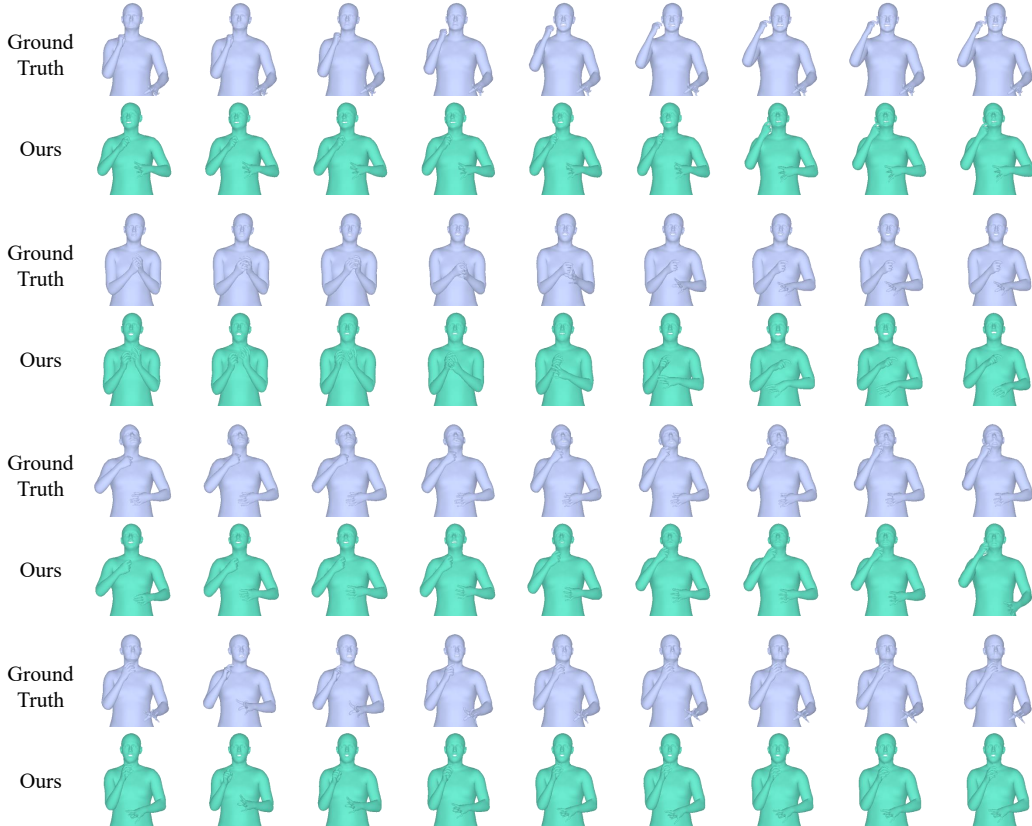


Figure 16: Qualitative results of *BRAID*. We compare the synthesized motions of our model (green) with the ground truth sequences (blue), demonstrating that our method accurately generates realistic and highly aligned sign language gestures.

I.2 Isolated-to-Continuous Signing

Ablation Studies of Training Components. Table 17 ablates the training components of *BRAID*. Without the proposed training stabilizers, the model shows a large vertex-level error despite a reasonable joint-level error, suggesting unstable reconstruction of fine-grained motion. Min-SNR weighting and EMA substantially reduce DTW-MPVPE, indicating that noise-level reweighting and parameter averaging stabilize diffusion training. Inpainting supervision alone improves DTW-MPJPE, but is less effective for vertex-level accuracy, suggesting that boundary-focused supervision benefits trajectory alignment but requires stable diffusion training to improve detailed motion. The full configuration achieves the lowest DTW-MPJPE and DTW-MPVPE.

Table 18 reports the effect of varying the depth of the hand-specific MLP in the part-wise motion head. Performance improves as the depth increases up to $\times 4$, which achieves the lowest DTW-MPJPE and DTW-MPVPE in both hand and overall metrics. This suggests that additional hand-specific capacity is beneficial for modeling fine-grained manual articulation. However, increasing the depth further to $\times 5$ degrades performance, indicating that excessive depth does not provide additional benefit and may reduce prediction stability. Based on these results, we adopt the $\times 4$ configuration.

Qualitative Results. Fig. 16 shows qualitative comparisons between the generated motions from *BRAID* and the ground-truth continuous signing sequences. Overall, the generated motions closely follow the reference sequences in terms of body posture, arm configuration, and hand trajectory. Across different examples, our model preserves the relative position of the dominant hand with respect to the torso and face, while also producing temporally coherent transitions between neighboring frames. These results suggest that *BRAID* can effectively refine the boundary region between isolated signs and recover continuous signing motions that are well aligned with the ground truth.

At the same time, we observe minor artifacts in some cases, particularly around the non-dominant hand. For example, the overall arm position remains consistent with the reference, but fine-grained hand shape or finger articulation can be slightly distorted. This indicates that while *BRAID* captures the global motion structure and

Table 17: Ablation study on *BRAID* training components.

Min-SNR	Inpaint	EMA	DTW-MPJPE ↓	DTW-MPVPE ↓
			0.0698	0.4685
✓			0.0708	0.0476
	✓		0.0670	0.0881
		✓	0.0716	0.0493
	✓	✓	0.0695	0.0472
✓		✓	0.0670	0.0462
✓	✓	✓	0.0653	0.0439

Table 18: Quantitative results with different hand depths.

	DTW-MPJPE ↓			DTW-MPVPE ↓			
	Body	Hand	Overall	Body	Hand	Face	Overall
×1	0.0414	0.14544	0.0693	0.0336	0.0178	0.0017	0.0470
×2	0.0427	0.1500	0.0702	0.0341	0.0185	0.0017	0.0478
×3	0.0421	0.14679	0.0691	0.0336	0.0189	0.0017	0.0470
×4	0.0376	0.1384	0.0653	0.0309	0.0171	0.0017	0.0439
×5	0.0419	0.14632	0.0691	0.0335	0.0193	0.0017	0.0469

<p>Spoken sentence: Do you usually talk with Jessica and Donna? What? Why?</p> <p>GT: IX-2p TEND CHAT WITH JESSICA AND DONNA DO-DO WHY</p> <p>Ours: IX-2p TEND CHAT WITH JESSICA AND DONNA WHAT WHY</p> <hr/> <p>Spoken sentence: My mother is still working.</p> <p>GT: IX-honorific POSS-1p MOTHER STILL WORK</p> <p>Ours: POSS-1p MOTHER STILL WORK</p> <hr/> <p>Spoken sentence: If I arrive to work late, my boss will fire me.</p> <p>GT: IF IX-1p ARRIVE WORK LATE POSS-1p BOSS FUTURE FIRED IX-1p</p> <p>Ours: IF IX-1p ARRIVE WORK LATE POSS-1p BOSS FUTURE FIRE IX-1p</p>
--

Figure 17: Qualitative examples of spoken-to-gloss translation.

co-articulatory transition well, accurately preserving detailed hand geometry remains a challenging aspect of 3D sign motion generation.

I.3 Spoken Language to Gloss

Qualitative Results. Fig. 17 presents qualitative examples of spoken-language-to-gloss translation. The model generally preserves the core meaning of the spoken sentence while producing compact gloss sequences. In the first example, it preserves the wh-question structure but realizes the reference DO-DO as WHAT, showing that plausible gloss alternatives may differ from the reference convention. In the second example, it omits the discourse-dependent marker IX-honorific while retaining the main meaning of “my mother is still working.” In the third example, the model correctly captures the conditional structure and event semantics, but generates FIRE IX-1p instead of the reference FIRED IX-1p. This indicates that the translator may favor a surface-aligned verbal form when the reference uses a convention-specific gloss form. Overall, the results suggest that our translator captures propositional meaning reliably, while fine-grained gloss conventions and context-dependent markers remain challenging.


I.4 Sign-to-Sign Conversation

I.4.1 Retrieval-Based Semantic Evaluation Method

We further evaluate whether sentence-level sign motions can recover their corresponding semantic annotations through the proposed hybrid retrieval protocol. This experiment is conducted on ground-truth assistant test motions as queries, and serves as an upper-bound calibration of the retrieval-based evaluator. Specifically, it measures how often the evaluator retrieves the corresponding reference sentence from the SIGNVOX-U memory and how closely the selected hybrid candidate matches the reference gloss annotation.

Evaluation metrics. We report retrieval accuracy using Recall@*k* and mean reciprocal rank (MRR). Recall@*k* measures whether the ground-truth sentence appears within the top-*k* retrieved candidates, and MRR measures the average reciprocal rank of the ground-truth sentence. We report these as R@1, R@5, R@10, and MRR. To evaluate semantic recoverability at the gloss level, we compare the gloss annotation of the final hybrid


Case #1

User 


3D sign input

I put in two quarters for a coke, but nothing came out of the machine.


signavox



Ground Truth



Case #2

User 

3D sign input

I want to start meal planning to reduce food waste. What are some basic steps I can follow?

signavox

To start, plan your meals for the week, make a grocery list, and shop for only what you need.



Ground Truth

That's a great goal. To start, plan your meals for the week, make a grocery list, and shop for only what you need. You can ...



Figure 18: Qualitative results of the SIGNAVOX conversational model. We compare the generated 3D sign responses (blue) with the ground truth (pink) based on the user’s input. Note that while the actual user input is provided as 3D sign features, it is displayed here as spoken language text for better readability. Additionally, the glosses corresponding to the SIGNAVOX outputs are predicted by our retrieval model (in Sec H.1).

retrieval result with the reference gloss sequence. We report token-level F1, BLEU-4, and chrF, denoted as Gloss F1, Gloss BLEU-4, and Gloss chrF, respectively.

Results. Table 12 shows the upper-bound calibration results on ground-truth assistant test motions. The evaluator retrieves the exact reference sentence at rank 1 for 41.5% of the queries, and the recall increases to 58.4% and 64.4% within the top-5 and top-10 candidates, respectively. The MRR of 0.495 indicates that the corresponding reference sentence is often ranked near the top of the retrieval list. The final hybrid retrieval output also achieves 0.479 Gloss F1, 0.305 Gloss BLEU-4, and 0.498 Gloss chrF, showing that the retrieved candidates preserve a meaningful amount of gloss-level semantic information. These results provide a calibrated reference point for applying the same evaluator to generated SIGNAVOX sentence motions.

I.4.2 Qualitative Results

Fig. 18 presents qualitative examples of SIGNAVOX. For interpretability, we visualize the glosses and text retrieved by our semantic proxy evaluation model above the generated motions; these annotations are not directly produced by SIGNAVOX. In Case #1, the model generates a concise response corresponding to **REALLY**, which matches the initial reaction in the ground-truth response. The generated motion also exhibits a similar upper-body pose and hand configuration, suggesting that the model can produce appropriate short conversational feedback from the preceding sign context. In Case #2, the model generates a longer informative response to a meal-planning question. Although the output is not identical to the reference, it covers the same main semantic content, including planning meals, making a grocery list, and shopping only for necessary items. The motion sequence remains coherent across multiple signs and visually follows a similar gesture progression to the ground truth. These results indicate that SIGNAVOX can generate contextually appropriate sign responses at different response lengths, from short reactions to longer instruction-like utterances.

Single-Frame Selection for Fingerspelled Letters

System Prompt

You are given a temporally trimmed sign language video clip of a single fingerspelled alphabet letter.

Select exactly one frame that best preserves the canonical handshape and visibility of the target letter.

Do not prefer preparation frames.

Do not prefer transition frames.

Do not prefer blurred motion frames unless no clearer articulation exists.

Guidelines:

- Prefer the frame where the handshape is most canonical and visually stable.
- Avoid preparation, transition, and release frames if a clearer articulation frame exists.
- If several frames are nearly identical, choose the best single representative frame.

Strict output rules:

- Output ONLY one integer: `frame_index`
- No explanations
- No brackets
- No extra text

Example output:

12

User Prompt

The target gloss label is "`gloss`".

This gloss is a single fingerspelled alphabet letter.

Choose exactly one frame index for the clearest and most representative articulation of the letter "`gloss`".

Guidelines:

- Prefer the frame where the handshape is most canonical and visually stable.
- Avoid preparation, transition, and release frames if a clearer articulation frame exists.
- If several frames are nearly identical, choose the best single representative frame.

Return only one integer:

`frame_index`

Each frame contains a visible red label in the bottom-left corner formatted as 'frame #NN'. Use those visible frame indices exactly. The valid frame index range is 0 to `frame_count - 1`.

Figure 19: Prompt used to judge single frame selection. Blue text denotes input variables.

J LLM Prompt

J.1 VideoLLM Prompt for Articulation Frame Selection

The VideoLLM prompts used for articulation-frame selection are shown in Fig. 19, 20, and 21.

J.2 GPT Evaluation Prompt for Spoken to Gloss Translation

We evaluate the quality of spoken-to-gloss translation using GPT-5.2 [54]. Beyond automatic metrics, we also employ LLM-based evaluation to assess aspects that are difficult to measure with surface-level matching alone. Specifically, the semantic score measures how well the generated ASL gloss preserves the meaning of the original spoken language utterance. The structure score evaluates how well the generated gloss follows the ASL grammatical ordering of Time–Topic–Comment. Both scores are rated on a five-point scale, and the evaluation prompt is shown in Fig. 22.

J.3 Spoken to Gloss Translation System Prompt

The system prompt used for spoken-language-to-gloss translation is shown in Fig. 23.

Contiguous Span Selection for Core Lexical Articulation

System Prompt

You are given a temporally trimmed sign language video clip.

Your task is to identify the contiguous temporal span that best preserves the core lexical articulation of the sign.

Select the earliest frame where the articulation begins and the latest frame needed to preserve the articulation.

Do not include extra preparation frames before the articulation starts.

Do not include idle or resting frames.

Do not include repeated hold frames after the articulation is completed.

Prefer the shortest contiguous span that still preserves the sign's lexical identity.

Avoid selecting only a single frame unless the articulation is truly instantaneous.

Stop the span immediately once the lexical articulation is completed.

Do not include frames that only maintain the final pose.

Strict output rules:

- Output ONLY two integers: start_frame,end_frame
- No explanations
- No brackets
- No extra text

Example output:

12,16

User Prompt

The target gloss label is "`gloss`".

Use the gloss label only as semantic context. Base your decision on the visible articulation in the video.

Select the start and end frame indices of the core lexical articulation for the sign "`gloss`".

Guidelines:

- Include all frames necessary to preserve the handshape, orientation, and motion progression of the sign.
- Return one contiguous articulation span, not scattered frames.
- If the sign is mostly static, return the shortest span that still preserves the canonical articulation.
- If the sign is defined by motion or direction change, include the full visible articulation phase rather than only the peak frame.
- Stop the span as soon as the lexical articulation is completed.

Return only two integers separated by a comma:

start_frame,end_frame

Each frame contains a visible red label in the bottom-left corner formatted as 'frame #NN'.

Use those visible frame indices exactly.

The valid frame index range is 0 to `frame_count - 1`.

Figure 20: Prompt for selecting the start and end boundaries of the core articulation in general sign language videos. Blue text denotes input variables.

Boundary Refinement for Proposed Lexical Articulation Span

System Prompt

You are reviewing a first-pass temporal span for a sign language video clip.

Your job is to correct the proposed span only if the boundaries are not tight enough.

Be especially careful about unnecessary frames near the end of the span.

If the final part only maintains the completed sign, repeated hold, or resting posture, remove it.

Check carefully:

- Is the proposed start too early because preparation frames are still included?
- Is the proposed end too late because repeated hold, resting, or post-articulation frames remain?
- Only move the end later if meaningful lexical articulation is clearly missing.

Prefer the tightest contiguous span that still preserves the sign's lexical identity.

Strict output rules:

- Output ONLY two integers: start_frame,end_frame
- No explanations
- No brackets
- No extra text

Example output:

12,16

User Prompt

The target gloss label is "gloss".

A first-pass model predicted this articulation span:

start_frame=candidate_start, end_frame=candidate_end

You are now shown a candidate-focused clip covering frames focus_start to focus_end.

The visible frame labels are still the original global frame indices from the full trimmed clip.

Review this focused clip and tighten the proposal if needed.

Your main goal is to remove unnecessary late frames.

Prefer trimming borderline late frames unless they clearly contribute new lexical information.

Questions to check:

- Does the start still include preparation that should be removed?
- Does the end still include repeated hold, resting, or post-articulation frames that should be removed?
- Does the end include frames that only maintain the completed sign?
- Only extend the span if lexical articulation is clearly missing.

Return the final corrected span as:

start_frame,end_frame

Each frame contains a visible red label in the bottom-left corner formatted as 'frame #NN'.

Use those visible frame indices exactly.

The valid frame index range is focus_start to focus_end.

Figure 21: Prompt for refining the start and end boundaries of the core articulation in sign language videos based on a candidate span. Blue text denotes input variables.

GPT Evaluation Prompt

System Prompt

You are a strict evaluator for English → ASL gloss prediction quality.
This is a reference-based evaluation. Compare predicted gloss to reference gloss.
Evaluate with exactly two perspectives.
Return JSON only with this schema:
{'semantic_score': <integer 1..5>, 'ttc_structure_score': <integer 1..5>, }

Guidelines:

- semantic_score: 1 means meaning is mostly wrong, 5 means meaning is fully preserved.
- ttc_structure_score: 1 means poor ASL Time-Topic-Comment ordering, 5 means strong TTC ordering.
- Judge structure as ASL gloss grammar quality, not English word order.

User Prompt

English sentence:
`spoken language`

Reference ASL gloss:
`Reference gloss`

Predicted ASL gloss:
`Predicted gloss`

Evaluate now and return JSON only.

Figure 22: Prompt used to evaluate spoken-to-gloss translation quality with GPT-5.2. Blue text denotes input variables.

English-to-ASL Gloss Translation Prompt

GRAMMAR RULES (for English → ASL Gloss)

0) Output format constraints (important)

- Output ONLY the gloss tokens in ONE LINE.
- Tokens are space-separated.
- Use UPPERCASE for content signs whenever possible (e.g., GO, SEE, HOUSE, EXCITED).
- Keep the dataset-style tokens when needed:
 - Pronouns / deixis: IX-1p, IX-2p, IX-3p, IX-loc
 - Possessives: POSS-1p, POSS-2p, POSS-3p
 - Fingerspelling / names: fs-A-B-C..., ns-..., ns-fs-A-B-C..., WORD (loan sign)
- Words/expressions in quotes (" ") are often names or special notation. When appropriate, prefer dataset-style name/spelling tokens.
- Avoid adding non-manual markers or grammatical annotations that are not in the simplified gloss set.

1) Prefer the canonical ASL ordering: Time + Topic + Comment (important)

- Time: put time indicators first (YESTERDAY, TODAY, TOMORROW, PASTNIGHT, NOW, RECENT-PAST, FINISH, BEFORE, AFTER).
- Topic: place the main noun/theme early (often the object or scene-setting element).
- Comment: what is said about the topic (typically includes the verb and predicate).

Examples:

- "I went to the library yesterday." → YESTERDAY LIBRARY IX-1p GO-TO
- "My friend, I see them." → FRIEND IX-1p SEE IX-3p

2) Topicalization (Topic/Comment) and adjective ordering

- Topics come first. Any description of the topic (adjectives, attributes) comes before the comment.
- Order descriptive details in a natural ASL-like sequence (often: category + attribute + size/degree).
- Example:
 - "I see a big orange cat." → CAT ORANGE BIG IX-1p SEE

3) Visual/causal/sequence organization: sign in the order you "see it"

ASL often prefers ordering that matches visualization:

3.1 Cause → Effect

- Express the cause before the effect.
- Example:

- "I feel calm when I go to the park." → PARK GO-TO FEEL CALM IX-1p

3.2 Real-time sequencing (chronological order)

- Arrange events in the order they happen.

Example:

- "I'm worried because my brother didn't call me after he left."
→ POSS-1p BROTHER LEAVE CALL-BY-PHONE-1p NOT CONCERN IX-1p

3.3 General → Specific (scene setting)

- Establish the broad setting first, then narrow down to details.

Example:

- "I am excited after moving to my new house in Virginia."
→ VIRGINIA HOUSE NEW MOVE FINISH EXCITED IX-1p

4) Tense: verbs stay base form; tense is set by time markers

- Do NOT conjugate verbs by tense (EAT covers ate/eats/eating/eaten).
- Use time indicators at the beginning to establish time.
- Use FINISH (or similar) to indicate completed/past events when appropriate.

5) Questions: WH-words tend to go at the end

- Place WHO / WHAT / WHEN / WHERE / WHY / WHICH / HOW at the end of the sentence.
- If emphasis is needed, WH-word may appear at both beginning and end, but default is end.

Example:

- "What is your name?" → POSS-2p NAME WHAT

6) Copula deletion: do not include "to be"

- English "am/is/are/was/were" is often omitted in ASL gloss.

Example:

- "He is tall." → IX-3p TALL

7) Negation: NOT/NONE usually follows what it negates

- Negative signs often come after the verb or phrase they negate.

Example:

- "I don't have any pets." → PET HAVE NOT

8) Indexing and referents (use IX- / POSS- consistently)

- Use IX-1p / IX-2p / IX-3p to represent pronouns (I/you/he-she-they).
- Use POSS-1p / POSS-2p / POSS-3p to represent possessives (my/your/his-her-their).
- Use IX-loc to point to locations when needed (there/here/that place).
- In this simplified gloss style, do NOT add locus indices like ":i/:j"; prefer IX-3p and IX-loc.

9) Directional/agreement verbs (simplified)

- Some meanings are naturally expressed with directional verbs (GIVE, TELL, ASK, SEND/MAIL, CALL-BY-PHONE).

```

- In simplified gloss, keep the verb as a single token (e.g., CALL-BY-PHONE)
  and represent participants with IX/POSS nearby if needed.

10) Fingerspelling / names / loan signs
- If a proper noun (person/place/organization) has no known lexical sign, use:
  - ns-fs-J-O-H-N / ns-fs-M-A-R-Y for name-like entities (common in datasets)
  - fs-... for general fingerspelling
- Use WORD for common loan signs (dataset style), when appropriate.
- Use fingerspelling (fs-...) to emphasize the exact spelling of a word,
  especially when you want the viewer to notice the letters clearly.
- For common English words that have no known lexical ASL sign
  - Example: ventriloquism → fs-V-E-N-T-R-I-L-Q-U-I-S-M

11) Keep it dataset-like: prioritize learnable, consistent gloss
- Prefer common/high-frequency gloss tokens over rare stylistic paraphrases.
- If multiple ASL word orders are possible, prefer the one that matches:
  1. Time first, then topic, then comment
  2. Cause→Effect
  3. General→Specific
- Avoid adding extra functional markers unless they are represented in the simplified gloss vocabulary.

OUTPUT REQUIREMENT:

Given an English sentence, output ONLY the ASL gloss on a single line.

```

Figure 23: Full system prompt for converting English sentences to ASL gloss, incorporating all grammatical and formatting rules. Blue text indicates input variables.